Biogeosciences, 20, 4339–4357, 2023
https://doi.org/10.5194/bg-20-4339-2023

Biogeosciences Open Access EGU

Mobilisation thresholds for coral rubble and consequences for windows of reef recovery

Tania M. Kenyon[1], Daniel Harris[2], Tom Baldock[3], David Callaghan[3], Christopher Doropoulos[4], Gregory Webb[2], Steven P. Newman[5], and Peter J. Mumby[1]

[1]Marine Spatial Ecology Lab, School of Biological Sciences, The University of Queensland, St. Lucia, Australia
[2]School of Earth and Environmental Sciences, The University of Queensland, St. Lucia, Australia
[3]School of Civil Engineering, The University of Queensland, St. Lucia, Australia
[4]Commonwealth Scientific and Industrial Research Organisation, St. Lucia, Australia
[5]Banyan Tree Marine Laboratory, Vabbinfaru, North Malé Atoll, Maldives

Correspondence: Tania M. Kenyon (tania.kenyon@uq.net.au)

Received: 11 January 2023 – Discussion started: 16 February 2023
Revised: 3 August 2023 – Accepted: 10 August 2023 – Published: 24 October 2023

Abstract. The proportional cover of rubble on reefs is predicted to increase as disturbances increase in intensity and frequency. Unstable rubble can kill coral recruits and impair binding processes that transform rubble into a stable substrate for coral recruitment. A clearer understanding of the mechanisms of inhibited coral recovery on rubble requires characterisation of the hydrodynamic conditions that trigger rubble mobilisation. Here, we investigated rubble mobilisation under regular wave conditions in a wave flume and irregular wave conditions in situ on a coral reef in the Maldives. We examined how changes in near-bed wave orbital velocity influenced the likelihood of rubble motion (e.g. rocking) and transport (by walking, sliding or flipping). Rubble mobilisation was considered as a function of rubble length, branchiness (branched vs. unbranched) and underlying substrate (rubble vs. sand). The effect of near-bed wave orbital velocity on rubble mobilisation was comparable between flume and reef observations. As near-bed wave orbital velocity increased, rubble was more likely to rock, be transported and travel greater distances. Averaged across length, branchiness and substrate, loose rubble had a 50 % chance of transport when near-bed wave orbital velocities reached 0.30 m s^{-1} in both the wave flume and on the reef. However, small and/or unbranched rubble pieces were generally mobilised more and at lower velocities than larger, branched rubble. Rubble also travelled further distances per day ($\sim$ 2 cm) on substrates composed of sand than rubble. Importantly, if rubble was interlocked, it was very unlikely to move ($<$ 7 % chance) even at the highest velocity tested (0.4 m s^{-1}). Furthermore, the probability of rubble transport declined over 3 d deployments in the field, suggesting rubble had snagged or settled into more hydrodynamically stable positions within the first days of deployment. We expect that snagged or settled rubble is transported more commonly in locations with higher-energy events and more variable wave environments. At our field site in the Maldives, we expect recovery windows for binding (when rubble is stable) to predominantly occur during the calmer north-eastern monsoon when wave energy impacting the atoll is less and wave heights are smaller. Our results show that rubble beds comprised of small rubble pieces and/or pieces with fewer branches are more likely to have shorter windows of recovery (stability) between mobilisation events, and thus be good candidates for rubble stabilisation interventions to enhance coral recruitment and binding.

1 Introduction

Coral reefs routinely experience disturbances that physically break up reef rock and live coral skeletons into fragments within the cycle of erosion and accretion (Scoffin, 1992, 1993; Blanchon and Jones, 1997; Blanchon et al., 1997). Some of these coral fragments reattach, contributing to asexual recruitment (Highsmith, 1982), while others die and contribute to the accumulation of rubble on the substrate, which is naturally high on some reefs (Thornborough,

2012; Davies, 1983). Disturbances, including storms, dynamite fishing, ship groundings and trampling, can cause large accumulations of rubble (Fox and Caldwell, 2006; Viehman et al., 2018; Gittings et al., 1994; Hawkins and Roberts, 1993; Scoffin, 1993; Woodley et al., 1981a). Coral bleaching and disease do not directly reduce structural complexity but result in in situ mortality and eventual breakdown of the coral skeleton into rubble (Scoffin and McLean, 1978; Aronson and Precht, 1997). As sea surface temperatures rise, storm and cyclone intensity is predicted to increase, particularly in the Atlantic and West Pacific (Meehl et al., 2007; Knutson et al., 2010), and bleaching events are becoming more frequent (Hughes et al., 2018; Hoegh-Guldberg, 1999). Reefs are predicted to "flatten" into systems with high rubble : coral ratios over time as recovery windows between disturbance events become increasingly smaller (Lewis, 2002; Hoegh-Guldberg et al., 2007; Alvarez-Filip et al., 2009). High rubble cover can persist in an unstable state for years to decades on some damaged reefs (Dollar and Tribble, 1993; Lasagna et al., 2008; Chong-Seng et al., 2014; Viehman et al., 2018; Fox et al., 2019) and can also form persistent rubble beds that remain for centuries to millennia (Liu et al., 2016; Clark et al., 2017; Yu et al., 2012; Montaggioni, 2005).

A key determinant of recovery on reefs where large tracts of coral have been turned to rubble is the stability of rubble. Rubble mobilisation correlates with flow velocity (Cheroske et al., 2000; Bruno, 1998; Viehman et al., 2018), wind speed and wave energy (Cameron et al., 2016), as well as in mesotidal regions with water depth, inundation duration and tidal phase (Thornborough, 2012). Hydrodynamic forcing above a certain threshold will cause rubble to be mobilised by sliding or flipping (Viehman et al., 2018). Moreover, the loss of structurally complex framework reduces a coral reef's capacity to dissipate hydrodynamic energy, leading to greater near-bed orbital flow velocities over rubble beds (Guihen et al., 2013). Frequent mobilisation events in a rubble bed can hinder the recovery of coral assemblages by increasing mortality of sexual and asexual coral recruits within the rubble bed through abrasion and smothering (Clark and Edwards, 1995; Brown and Dunne, 1988; Kenyon et al., 2020). Furthermore, mobilisation could break binds formed by encrusting organisms between individual rubble pieces, preventing the binding of rubble into a stable substrate (Rasser and Riegl, 2002). Rubble mobilisation under everyday wave conditions (as opposed to storm events) has resulted in a lack of recovery of coral assemblages over a period of 6 (Viehman, 2017) to 17 years (Fox et al., 2019) post-disturbance. Under future climate scenarios, sea level rise might also result in enhanced rubble mobilisation (Kenyon et al., 2023) via increased wave orbital velocities on some reefs (Baldock et al., 2014a, b). Implications of the persistence of rubble beds with low structural complexity extend beyond reduced coral cover, including reduced fish abundance, diversity and fishery productivity (Rogers et al., 2018; Luckhurst and Luckhurst, 1978; Graham et al., 2006), and reduced coastal protection (Harris et al., 2018a; Ferrario et al., 2014). To predict and manage the recovery potential of post-disturbance rubble beds, we must understand the drivers and frequency of rubble mobilisation.

Although disturbances attributed to hydrological regimes are well studied in some systems, e.g. substrate stability in streams and intertidal areas (Townsend et al., 1997; Suren and Duncan, 1999; Hardison and Layzer, 2001; Sousa, 1979), studies on rubble mobilisation on coral reefs are in their infancy. Sediment transport studies commonly deal with smaller particles than rubble, including sand, silt and clay (< 2 mm according to the modified Udden–Wentworth grain-size scale) (Blair and McPherson, 1999). As hydrodynamic energy increases, sediment from a larger range of size classes is transported (Komar and Miller, 1973; Kench, 1998b; Nielsen and Callaghan, 2003), in some cases on vast scales during cyclones and hurricanes (Keen et al., 2004; Hubbard, 1992). Attention has also been given to movement initiation of boulders from 20 kg to ~ 290 t (Nott, 1997, 2003; Nandasena et al., 2011; Etienne and Paris, 2010; Imamura et al., 2008; Kain et al., 2012). While coral rubble can be boulder-sized (Rasser and Riegl, 2002), clasts are typically much smaller, averaging 5–30 cm in length and as small as 1 cm (Highsmith et al., 1980; Fong and Lirman, 1995; Heyward and Collins, 1985; Dollar and Tribble, 1993; Kay and Liddle, 1989). Few studies have monitored mobilisation of rubble in this size range with knowledge of the wave environment and flow rate estimates, particularly in field environments (Cheroske et al., 2000; Viehman et al., 2018).

The probability that rubble will remain stable depends not only on hydrodynamic forcing but also on rubble characteristics (e.g. size and shape) and the type and bathymetry of the underlying substrate (the "pre-transport environment") (Nandasena et al., 2011; Nott, 2003). While their densities may vary slightly, research on the survivorship of live coral fragments provides insight into the behaviour of dead rubble pieces. Studies show that the likelihood of coral fragment survival decreases with decreasing size (Smith and Hughes, 1999), likely due to increased mobilisation of smaller fragments (Hughes, 1999). Fragments with non-branching morphologies have reduced survival compared to those with branching morphologies (Tunnicliffe, 1981; Heyward and Collins, 1985; Smith and Hughes, 1999), likely due to greater mobility and increased smothering of less complex shapes. The stability and survival of fragments also vary with substrate type and bathymetry. Live fragments tend to survive more commonly on rubble than on sand substrates (Heyward and Collins, 1985; Bruno, 1998; Bowden-Kerby, 2001; Prosper, 2005; Kenyon et al., 2020) and are transported further in reef slope zones where gravity assists mobilisation than in planar lagoons with low slope angles (Smith and Hughes, 1999). Steep slopes can foster downslope transport and the formation of a rubble talus (Rasser and Riegl, 2002; Dollar and Tribble, 1993). Rubble beds on reef slopes generated by intense disturbances and comprising small, unbranched rubble are therefore likely at high risk of mobilisation. However,

to our knowledge there has been no study where the threshold of mobilisation for individual rubble pieces of varying shapes and sizes, and on different substrate types and slopes, has been empirically determined in both controlled and field settings.

Here, we report how the probability of rubble mobilisation changes as near-bed wave orbital velocity increases under average (everyday) hydrodynamic conditions. We quantified the thresholds required to mobilise coral rubble and identified effects of rubble size and morphology, underlying substrate type, and slope angle, on the likelihood of mobilisation. Experiments were conducted in a controlled, wave flume environment and replicated as closely as possible in the field to extend findings from a regular (monochromatic) wave environment to an irregular wave environment. We hypothesised that the probability of rubble mobilisation would decrease as (i) rubble size increases, (ii) morphological complexity increases (of both the rubble and of the substrate type), and (iii) the slope angle decreases (and the contribution of gravity subsequently decreases). Managers of reefs that exhibit a significant increase in rubble cover can use the mobilisation estimates reported here, coupled with knowledge of the reef's hydrodynamic exposure (e.g. publicly accessible wind data, wave climate estimates), rubble typology and other environmental factors, to predict the frequency of everyday rubble mobilisation and the likelihood of natural rubble stabilisation and recovery.

2 Methods

2.1 Mobilisation in flume

To determine the velocity required to mobilise rubble, trials were conducted in a wave flume (l: 20; w: 2; d: 1.2 m) using a DHI Technologies piston wave maker (Fig. 1a–b; see Baldock et al., 2017, for general description). Cylindrical rubble pieces (from branching coral species) were collected from Lizard Island, Great Barrier Reef, in 2017 after the 2016 bleaching event. Rubble was divided into four size categories based on axial length (4–8; 9–15; 16–23; and 24–36 cm; all with a diameter of 1–2 cm) and two "branchiness" categories: unbranched (if rubble had no branches > 1 cm length) and branched (if rubble had branches > 1 cm length), with 5–10 pieces in each size/branchiness group. The size range of rubble used in the laboratory phase of the study is consistent with that commonly observed on reefs following natural and anthropogenic disturbances (Highsmith et al., 1980; Fong and Lirman, 1995; Heyward and Collins, 1985; Dollar and Tribble, 1993), as well as the size range (1–27, mean 7 cm) of 440 rubble pieces measured from Vabbinfaru Reef (which also suffered bleaching in 2016) where the field portion of this study was undertaken.

The mobilisation of "loose" (not interlocked) cylindrical rubble was tested on two substrate types: sand and rubble. Beach sand ~ 2 cm (grain size $d_{50} = 0.28$ mm) deep was spread over the flume base to form the sand substrate (Fig. 1a). The rubble substrate comprised "Serenity Aquatics" coral rubble (l: 3–5 cm) glued to a plywood base (l: 2; w: 1 m) that lay on the concrete base of the flume (Fig. 1b). The mobilisation of interlocked rubble was tested on a second rubble substrate, which comprised a stainless-steel mesh with rubble of mean length 9 cm (3–20 cm range) attached with cable ties (Fig. S1). The height of both bases averaged 2 cm, although some rubble pieces protruded up to 5.5 cm in the second base. Small- and medium-sized branched cylindrical rubble of 4–15 cm length was manually interlocked with the second rubble base prior to testing. Larger rubble and unbranched rubble could not be suitably interlocked and therefore were not tested on the second rubble base.

Rubble was placed along a reference line parallel with the wave paddle, with the long axis normal (perpendicular) to flow to identify the minimum velocity threshold (short-axis normal to flow requires a higher threshold) (Fig. 1a–b). The wave maker ran 30 s bursts of regular (monochromatic) waves, starting at water depth $(h) = 0.42$ m, wave height $(H) = 0.05$ m and wave period $(T) = 1$ s. Wave height (H) was increased in 0.02 m increments at the same period (T). Three replicate waves were run for each wave height and period combination, and the movement type for each rubble piece was recorded for each run. Binding could be prevented and weak binds damaged by even small rocking motions, and corals could be abraded and smothered by rubble transport and flipping. Thus, the movement categories chosen were the following: no movement (rubble remained stable and in the same position); rocking (rubble rocked back and forth and in some cases rotated, but remained in the same position); transport by walking/sliding (rubble walked/skittered or slid away from initial position); and transport by flipping (rubble overturned at least once). If a piece rocked, then slid and then flipped within one run, the movement type was marked as flipping, because more force is required to overturn a piece than to rock or slide it (Viehman et al., 2018; Imamura et al., 2008). The near-bed wave orbital velocity ($\mathrm{m\,s^{-1}}$) for each run was estimated using the Soulsby cosine approximation (Soulsby, 2006), shown to produce similar estimates to linear wave theory (within $0.01\ \mathrm{m\,s^{-1}}$) (Fig. S2, Table S1).

To determine whether scaling effects were necessary to compare velocity thresholds between flume and field conditions, we derived a relationship for the contribution of the inertia force to the total maximum force as a proportion of the drag force, for all wave conditions tested. Total force depends on both the inertia force and drag force components, and while the inertia component is dependent on velocity and wave period, the drag component is solely dependent on velocity (Table S1). Thus, where conditions are determined to be drag dominated, rubble movement depends primarily on velocity, and valid comparisons between flume and field can be made despite their variance in wave period. The contribution of inertia force to the total maximum force for each

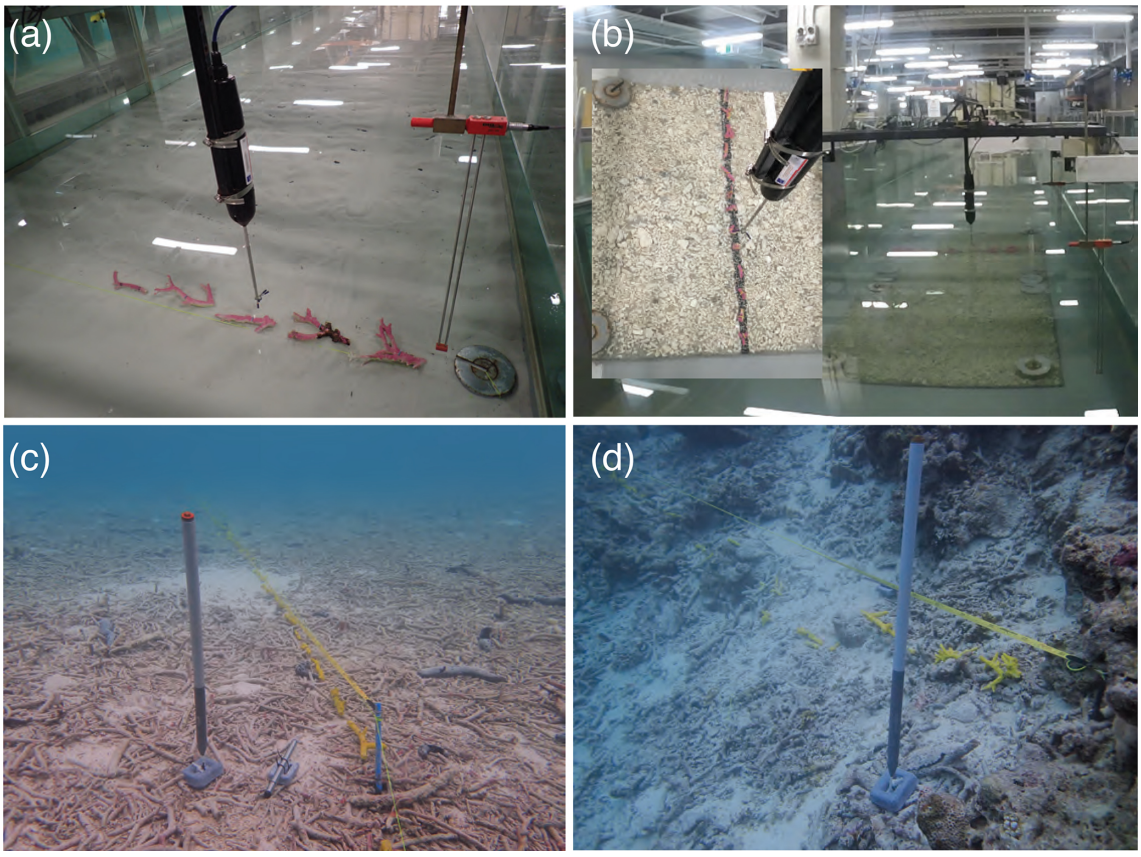

Figure 1. Experimental rubble (painted) lined up along a reference line **(a)** in flume with sand substrate, **(b)** in flume with rubble substrate to test loose pieces and inset close-up view, **(c)** in the field in a shallow reef flat site (2–3 m), and **(d)** in the field in an exposed deep site (6–7 m, western reef) (source: Tania Kenyon).

wave height and period combination in the flume, based on an average coral diameter of 1.64 cm (range ∼ 1–2 cm), is shown in Table S1. Only 19 out of 71 wave conditions in the flume have the potential for the inertia force to be significant, and of those, only 7 had a $\frac{F_I}{F_D}$ ratio > 2, meaning that nearly all wave conditions in the flume led to drag-dominated conditions. Furthermore, the inertial component decreases as velocity increases (Fig. S5), and inertial forces were negligible at the 50 % and 90 % transport thresholds (see results for further explanation). The flume and field experiments are therefore comparable without scaling effects.

2.2 Mobilisation in field

To compare flume trials to a natural reef setting, trials were conducted in the field across different reef zones on Vabbinfaru Reef, North Malé Atoll, Maldives (4°18′35″ N, 73°25′26″ E). The reef crest is 0.6–1.5 m below mean sea level and surrounds a shallow subtidal reef flat (∼ 1.17 m below mean sea level) and sand cay (Morgan and Kench, 2012). Tidal ranges in the region are microtidal: 0.6 and 1.2 m during neap and spring tides, respectively (Kench et al., 2009). When this study was conducted, rubble cover was high on the reef flat and on the reef slope following bleaching events in 1998 and 2016 (Zahir et al., 2009; Perry and Morgan, 2017). Coral cover on the reef crest was reduced from 50 %–75 % down to 9 % (Banyan Tree Marine Laboratory, unpublished data). The Maldives has two distinct monsoon seasons: the wet from April to October, during which stronger winds blow predominantly from the south-west, and the dry from November to March, where north-eastern winds are gentler on average (Kench et al., 2006, Fig. S3). The north-eastern and western monsoons correspond to minimum and maximum incident ocean swell conditions, respectively (Kench et al., 2009). Daily winds at Vabbinfaru average 10 kn (mean daily maximum 19.8 kn) and are predominantly westerly, while the south-east region of the reef is relatively sheltered year-round (Fig. 2b) (Beetham and Kench, 2014).

Previous studies on Vabbinfaru reef suggest that sediment transport is largely controlled by wind-driven waves associated with the western monsoon, rather than tidally driven currents (Morgan and Kench, 2014a). Thus, rubble mobilisation was related to near-bed wave orbital velocity. To capture a gradient in wave energy, rubble mobilisation was tracked in different sites and monsoon seasons. Fifteen field sites were

delineated across reef flat (∼ 2 m depth), shallow reef slope (2–3 m) and deeper reef slope (6–7 m) environments on the sheltered (south-east) and comparatively exposed (western) sides of the island (Fig. 2a). The field trials were conducted in all sites in the north-eastern monsoon (late November 2017 to January 2018) and again in the western monsoon (early August to September 2018).

The wave environment in each of these sites and seasons was characterised using INW Aquistar® PT2X 30 PSIA pressure loggers placed on the seabed and recording continuously at 2 Hz (Fig. 1c). Using known processing methods (Harris et al., 2015, 2018b), records from the pressure loggers were low-pass filtered to remove instrument noise and high-pass filtered to remove infragravity effects (at 0.05 Hz) and then split into 30 min runs to remove tidal influence (Hughes and Moseley, 2007). Pressure was converted to depth, and wave spectra for each 30 min run were calculated between 0.0033–0.33 Hz using the Welch method for computing power spectral densities from 3600 sample records, to obtain significant wave height (H_s) and peak wave period (T_p). The near-bed wave orbital velocity (U) was then estimated for each 30 min run using linear wave theory using Eq. (1).

$$U = \frac{H_s}{2\sin h(kh)} \cdot \frac{2\pi}{T_p} \quad (1)$$

Here the wave number (k) was determined by solving Eq. (2).

$$\varpi^2 = gk\sin h(kh) \quad (2)$$

Here ω is the wave radian frequency ($2\pi/T_p$), h water depth and g the acceleration due to gravity.

The contribution of the inertia force to the total maximum force as a proportion of the drag force was estimated for each H_s and T_p combination used in the field analysis, based on an average coral diameter of 1.69 cm (range ∼ 1–3 cm) (Table S2). Only 1 out of 90 wave conditions in the field had the potential for inertia to be significant, meaning that most conditions in the field were drag-dominated. Furthermore, this one condition corresponded to a very low velocity ($0.016\,m\,s^{-1}$), far from the reported 50 % and 90 % transport threshold velocities.

Rubble movement was tracked while the wave environment was measured, to correlate rubble mobilisation with near-bed wave orbital velocity. At each site and in each season, ∼ 20 marked (painted yellow) rubble pieces of axial length category 4–8 cm, ∼ 20 pieces 9–15 cm and ∼ 10 pieces 16–23 cm of both branched and unbranched varieties were placed along and directly beneath a reference string strung parallel to the reef crest (Fig. 1c–d). A black dot was painted on the underside of each piece. The substrate beneath the rubble was recorded as either sand, rubble or hard carbonate, and the slope angle was measured at 50 cm intervals along the reference string using a spirit level and right-angle set square. As the depth on the reef slope likely excluded swash effects, the net direction of mobilisation was expected to be downslope aided by gravity, rather than upslope with wave direction. Mobilisation direction on the reef flat, however, was expected to be shoreward. Generally, reef flat sites were characterised by flatter slopes, shallow reef slope sites by gentle slopes and deeper reef slope sites by steeper slopes (Fig. 1c–d). The perpendicular distance from the reference string to each rubble piece was recorded over 3 d, approximately 24, 48 and 72 h after deployment. A transect tape was laid along the reference string to also record the point along the tape with which the rubble piece aligned. These two measurements were used to calculate the diagonal distance travelled by the rubble piece during each 24 h interval over 3 d. Whether or not the piece rotated or flipped was also recorded (if ≥ 50 % of the black dot was visible). A piece was only considered to have moved if it was > 1 cm from its starting point. This buffer provided a degree of conservatism to account for possible variations in the angle of gaze looking down on the reference string. Rocking movements could not be recorded in situ as rubble pieces were not continually observed.

From the 30 min runs across each 3 d period and site (144 each period and site), the fastest wave orbital velocity (calculated from significant wave height and peak wave period) was selected for each day, to regress with observed rubble movement on that day. A total of the 90 fastest wave orbital velocities were thus used in the analyses that included all 3 d (1 velocity per day × 3 d × 15 sites × 2 seasons), and 30 were used in the analyses that included the first day only (1 velocity for each "day 1" × 15 sites × 2 seasons).

2.3 Statistical analyses

The movement categories of rocking, transport and flipping (in the flume), and transport and flipping (in the field) were modelled as binary (Bernoulli) responses and classed as either a "0" or a "1" depending on the analysis (Table 1). For example, when modelling the probability of transport in the flume, rubble was classed as "0" if it did not move or rocked only and "1" if it walked/slid or flipped. Movements of walking, sliding and flipping were considered in this case in order to compare mobilisation thresholds across flume and field (transported rubble in the field could have moved by any of these three movement types) (Table 1). Similarly, when modelling the probability of flipping in the flume, rubble was classed as "0" if it did not move, rocked or walked/slid and as a "1" only if it flipped. All analyses were conducted in R (R Core Team, 2020). For all models, backwards step-wise selection was used to remove non-significant terms, whereby reduced models were compared to full models using the corrected Akaike information criterion (AICc) with the package "MuMIn" (Bartoń, 2020). Model assumptions were assessed using diagnostic plots.

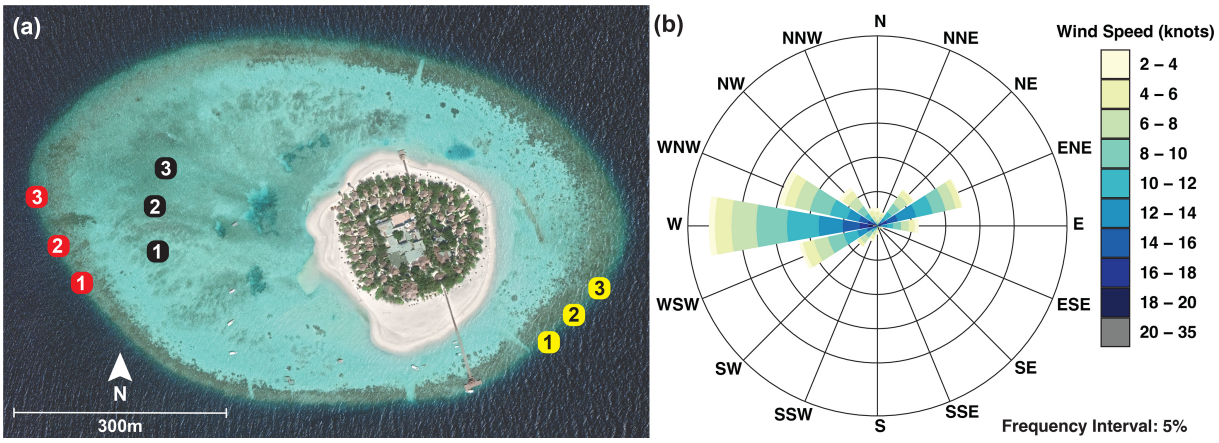

Figure 2. (a) Field sites at Vabbinfaru platform: three 2–3 m sites on the reef flat (black); three site locations on the exposed western reef slope (red), each comprising a shallow (2–3 m) and deep (6–7 m) site; and three site locations on the sheltered south-east reef slope (yellow), each comprising a shallow and deep site (source: ©Google Earth). **(b)** Wind rose of mean wind speed (knots) and wind direction data measured at nearby Hulhumale ranging 1985–2018 for both seasons (data source: Maldives Meteorological Service, Government of Maldives).

Table 1. Rubble movement types associated with each type of analysis from flume observations (i.e. probability of rocking, transport and flipping for loose, not interlocked, cylindrical rubble) and the analysis from field observations to which each was compared.

Flume analyses	Movement types classed as "0"	Movement types classed as "1"	Comparison to which field analyses
Rocking	No movement	Rocking (all other movement types excluded for this analysis)	n/a (rocking could not be distinguished in the field as rubble was not observed continuously).
Transport	Rocking or no movement	Walking/sliding; or Flipping	Transport > 1 cm
Flipping	Walking/sliding, rocking or no movement	Flipping	Flipping

n/a stands for not applicable.

The probability of flipping alone may have been underestimated in the field; i.e. a rubble piece might have rolled a complete 360°, meaning the black dot was again on the underside and not visible at the time of observation. Thus, the most appropriate comparison of mobilisation thresholds in the flume and field was between the threshold of transport in the flume for loose (not interlocked) cylindrical rubble and the threshold of transport in the field.

2.3.1 Mobilisation in flume

To identify the effects of rubble and substrate characteristics on the mobilisation of loose (not interlocked) rubble, logistic regression models (glm) were run using the base R "stats" package, with the type of movement as the response variable and velocity, rubble size, branchiness, substrate and all interaction terms up to third-order interactions as explanatory variables. The analysis of the probability of rocking only considered trials where rocking (no transport) was the greatest movement observed. Interactions were investigated by conducting pairwise comparisons across levels of factors at velocities of 0.1, 0.2, 0.3 and 0.4 $m\,s^{-1}$ using the "emmeans" package with Tukey adjustment (Lenth, 2020). It is expected that rubble beds in situ contain a variety of shapes and sizes of pieces and span multiple substrate types. Thus, to determine the threshold velocities at which 50 % and 90 % of rubble are transported, averaged across all rubble sizes, shapes and substrates, a reduced model was run with the type of movement as the response variable and "velocity" as the sole explanatory variable. This model only used data for rubble of lengths ranging 4–23 cm (no 24–39 cm size class), to be consistent with the range of rubble used in the field and thus make thresholds comparable.

The mobilisation of interlocked rubble was analysed separately, and logistic regression models included "any movement" (movement types were combined due to low mobilisa-

tion observations) as the response variable and velocity, rubble size and a velocity–size interaction as explanatory variables. To determine the most common movement types for interlocked rubble, another model was run using "any movement" as the response variable, velocity, rubble size, movement type and interactions as explanatory variables (although only movement type remained in the model).

2.3.2 Mobilisation in field

To firstly characterise near-bed wave orbital velocities for each habitat and season, the package "glmmTMB" (Brooks et al., 2017) was used to fit a mixed-effects model with a gamma distribution, with the fastest near-bed wave orbital velocity ($m\,s^{-1}$) as the response variable. Due to the lack of deep sites on the reef flat, leading to an unbalanced design, aspect and depth were combined to form a new variable "habitat". Habitat was then fit as an explanatory variable together with season and interactions. Sites within the deployment date were included as random effects.

To determine how the relationship between velocity and mobilisation varied across the 3 d period in each season, two mixed-effects models with binomial distributions were fit using the package "glmmTMB", with rubble transport > 1 cm as the response variable (0 or 1) and near-bed wave orbital velocity and day and their interactions as explanatory variables. Each rubble pieces' unique ID, within the site within the deployment date, was included as a nested random effect. A third and fourth model were fit with identical explanatory variables and random effects, but with the probability of flipping as the response variable for each season. A fifth and sixth model were fit using the package "nlme" (Pinheiro et al., 2019), utilising a gamma distribution and the same explanatory variables but with "distance transported by rubble" as the response variable for each season. The response variable was logged to achieve normality. Only rows for which rubble was transported ≥ 1 cm were retained (i.e. zeroes removed), and due to this reduction in replication, the only random effect retained for these models was site.

To determine mobilisation thresholds in the field and investigate the effects of rubble and substrate characteristics on mobilisation, only data from day 1 were used. This is because the conditions from day 1 in the field were most like flume conditions, as rubble had been newly deployed and had no opportunity yet to settle. Furthermore, mobilisation in the field was modelled against the full range of velocities pooled across habitats and seasons. A model was fit using the package "glmmTMB" with the probability of transport > 1 cm as the response variable and velocity, rubble size, branchiness, substrate and all interactions as explanatory variables. Site was included as a random effect. A second model was fit with identical explanatory variables and random effect, but with the probability of flipping as the response variable. To provide a valid comparison to the transport thresholds in the flume, reduced models with velocity as the sole explanatory variable were fit to determine the 50 % and 90 % thresholds for transport > 1 cm and flipping, averaged across all rubble sizes and substrates. To investigate the distance transported by rubble on day 1, a third model was fit using the "nlme" package with distance as the response variable and velocity, rubble size, branchiness and substrate as explanatory variables. No interactions were fit due to low replication of rubble pieces that had moved distances > 1 cm. Site was included as a random effect.

Slope was included in each of the three models above but was found to be consistent across rubble size, branchiness and substrate; i.e. there were no interactions with slope when included in full models. Thus, three additional models were fit with only velocity, slope and the velocity–slope interaction as explanatory variables, with movement type as the response variable and site as the random effect.

3 Results

3.1 Mobilisation in flume

3.1.1 Loose rubble – mobilisation thresholds

When averaged across rubble of sizes 4–23 cm, morphologies and substrates, we found that half of all rubble experienced rocking motions when velocities reached $0.28\,m\,s^{-1}$ (SE: 0.005), and 90 % of rubble rocked at $\geq 0.48\,m\,s^{-1}$ (SE: 0.013). At these higher velocities, pieces were less likely to rock and more likely to be transported or flipped. The 50 % and 90 % mobilisation thresholds for rubble transport (walk/sliding/flipping) were slightly higher: $0.3\,m\,s^{-1}$ (SE: 0.003) and $0.43\,m\,s^{-1}$ (SE: 0.006), respectively (Table S3). Near-bed wave orbital velocities had to reach $0.34\,m\,s^{-1}$ (SE: 0.004) for 50 % of rubble to flip completely and $0.5\,m\,s^{-1}$ (SE: 0.009) for 90 % of rubble to flip (Table S4).

In addition to calculating the inertia component for each wave height and period combination in the flume based on the average coral diameter (see Sect. 2.1: Methods), we also made these calculations for individual runs using the unique diameter of each piece. Of the cases identified as having the potential for inertia forces to be significant, the majority were runs where rubble did not move. Further, 9.3 % (195 of 2081) were runs where only rocking movements were recorded. The highest velocity represented in these cases was $0.2\,m\,s^{-1}$, though the majority were much lower (Fig. S6). Thus, at velocities $< 0.2\,m\,s^{-1}$, there is the potential for inertia forces to contribute to causing rocking motions. But, at a velocity of $0.2\,m\,s^{-1}$, the contribution of inertia is still only 25 % of the drag force (not dominant), and the threshold of rocking conditions in the flume, reported above, is drag dominated.

Transport or flipping occurred in only 0.9 % of runs where we determined inertia forces to be potentially significant (18 of 2081 runs) (Fig. S7). For these cases, the average contri-

bution of inertia forces to the total force was 36 % of the drag force, and the highest velocity represented in these cases was $0.16\,m\,s^{-1}$ (Table S7). This indicates that, at low velocities $< 0.16\,m\,s^{-1}$, there is the potential for inertia forces to be significant. However, this cut-off is well below the 50 % and 90 % thresholds of transport reported above, and at those velocities the inertia component contributes as little as 0.1 % and at most 4.9 % to the total force. The thresholds of transport conditions in the flume are thus drag dominated.

3.1.2 Loose rubble – rubble and substrate effects on mobilisation

Probability of "rocking"

Rubble was more likely to rock as velocity increased, but the relationship varied with rubble size, shape and underlying substrate (Fig. 3). Consequently, there were three-way interactions among velocity, size and branchiness ($\chi^2 = 55.3$, $P < 0.001$) and among velocity, size and substrate ($\chi^2 = 17.8$, $P < 0.001$) (Table S5). The branchiness of rubble was an important predictor of rocking. Across all velocities, rubble of all size classes was more likely to rock if they were unbranched rather than branched (except for intermediate rubble 16–23 cm, Fig. 3ai–iv) (Table S6). Once a velocity threshold was exceeded, rubble size and substrate also played a part. For velocities $\geq 0.2\,m\,s^{-1}$, the rocking of smaller rubble (4–8 and 9–15 cm) was sensitive to the underlying substrate, being more likely to rock on sand than rubble (Fig. 3ai–iv) (Table S7). Once velocities exceeded $0.3\,m\,s^{-1}$, the smallest rubble pieces (4–8 cm) were more likely to rock than all larger-sized rubble (Table S8), averaged across substrate types.

Probability of "transport" (walk/slide/flip)

As with rocking movements, the probability of transport also increased with velocity, depending on rubble characteristics and substrate, again with two three-way interactions (velocity, size and branchiness $\chi^2 = 17.6$, $P < 0.001$; velocity, size and substrate $\chi^2 = 8.9$, $P < 0.03$) (Table S9). Qualitatively, the patterns for transport were similar to those for rocking, but the effect of branchiness changed at high velocities. For example, unbranched rubble was transported more commonly than branched rubble at velocities $\leq 0.4\,m\,s^{-1}$, after which rubble of both morphologies was equally as likely to be transported, at least for sizes 4–8 and 16–23 cm (Fig. 3bi–iv) (Table S10). Size was a clear predictor of transport, with 4–8 cm rubble more likely to be transported than two groups of larger rubble: 16–23 and 24–39 cm, at velocities $\geq 0.2\,m\,s^{-1}$ (Table S11). There was even greater delineation of size if rubble was branched; 4–8 cm branched rubble was more likely to be transported than *all* larger rubble at velocities $\geq 0.3\,m\,s^{-1}$, on both substrates (Fig. 3biii–iv, Table S11). Just as 4–8 cm rubble rocked more easily on sand, it also tended to be transported more easily on sand at velocities $\geq 0.3\,m\,s^{-1}$. Interestingly, the largest rubble pieces 24–39 cm were more likely to be transported on rubble than on sand at these velocities (Table S12), perhaps due to an ability to sink into sand but not rubble.

Probability of "flipping" only

We distinguish flipping on its own, because it is the form of transport expected to involve some form of abrasion across most surfaces of the rubble. Like rocking and transport probabilities, two three-way interactions affected the probability of flipping (velocity, size and branchiness $\chi^2 = 18.4$, $P < 0.001$ and velocity, size and substrate $\chi^2 = 10.7$, $P = 0.013$; Table S13). Again, unbranched rubble was more likely to flip than branched rubble (Fig. 3ci–iv; Table S14). Yet, branched, small 4–8 cm rubble was much more likely to flip than all larger rubble, particularly at velocities $\geq 0.4\,m\,s^{-1}$. Once again branchiness had a strong influence on this relationship, with unbranched rubble pieces having instead *similar* probabilities of flipping across a size range of 4–15 cm (Fig. 3ci–ii) (Table S15). Substrate type had little effect on rubble flipping. However, when pieces started to flip at $0.2\,m\,s^{-1}$, branched rubble flipped more on rubble substrate than on sand, while unbranched rubble was just as likely to flip on rubble or sand (Table S16).

3.1.3 Interlocked rubble

Rubble mobilisation trials were profoundly different when the experimental rubble was interlocked with the second rubble substrate. For interlocked rubble, there was no relationship between velocity and the probability of any type of movement (Table S17). Rubble was very unlikely to move (< 7 %) even at the highest velocity tested ($0.4\,m\,s^{-1}$). Yet while the probability of any movement was low, when interlocked rubble of both sizes *did* move they most commonly rocked (5 ± 1 %, mean ± SE) as opposed to being transported (1 ± 0.3 %) or flipped (1 ± 0.3 %) (rock vs. transport: z ratio = 3.671, $P < 0.001$; rock vs. flip: z ratio = −3.671, $P < 0.001$) (Table S49, Fig. S9). In fact, interlocked 4–8 cm rubble was not observed to walk, slide or flip at all.

3.2 Mobilisation in field

3.2.1 In situ environment

During deployment periods, higher significant wave heights were recorded in the western monsoon compared to the north-eastern monsoon (Table 2).

Corresponding near-bed wave orbital velocities also were significantly higher in the western monsoon than in the north-eastern monsoon, except for reef flat and exposed shallow slope sites (despite a trend, Fig. 4, Tables S18, S20).

Consequently, there was an interaction between season and habitat on near-bed wave orbital velocity ($\chi^2 = 102.2$,

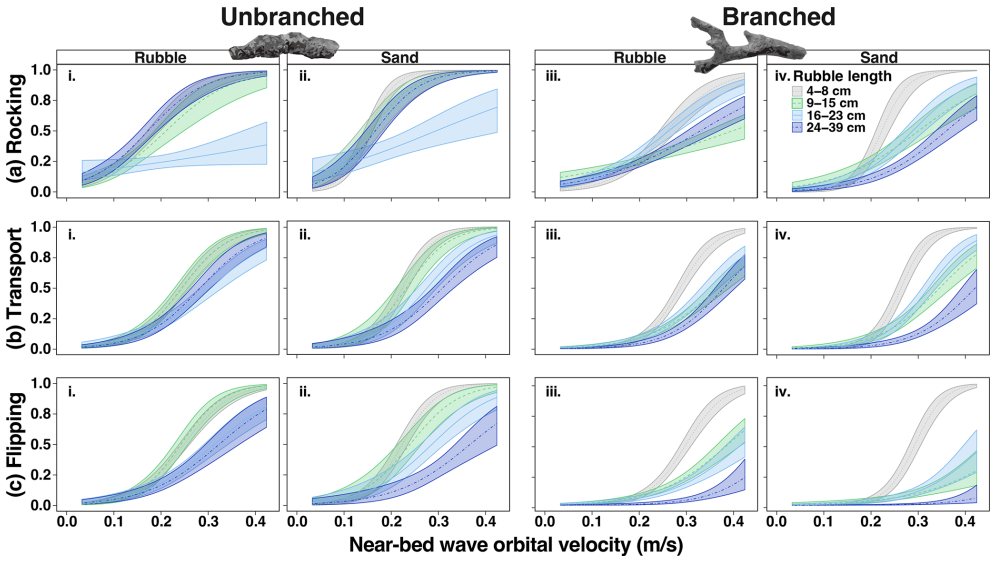

Figure 3. The probability of **(a)** rocking, **(b)** transport and **(c)** flipping with increasing near-bed wave orbital velocity for branched and unbranched rubble of four size categories (grey: 4–8 cm; green: 9–15 cm; light blue: 16–22 cm; dark blue 24–39 cm) on rubble and sand substrates. Note that, at low velocities $< 0.2\,\mathrm{m\,s^{-1}}$, we estimate there is the potential for inertia forces to contribute to causing rocking motions; at velocities $< 0.16\,\mathrm{m\,s^{-1}}$, there is the potential for inertia forces to contribute to causing transport and flipping.

Table 2. Wave statistics for each habitat (aspect and depth) and monsoon season. Reef flat and western sites are on exposed aspect; south-east sites are on sheltered aspect. Mean statistics show average of all 30 min runs in the 3 d period across 3 sites on the reef flat and 6 sites on sheltered and exposed reef slope (15 sites total). Max statistics show the highest of the 30 min runs. H_s denotes significant wave height; T_p denotes peak wave period.

Monsoon season	Depth	Aspect	Mean H_s (m)	Max H_s (m)	Mean T_p (s)	Max T_p (s)
North-east	2–3 m	Reef flat	0.08	0.21	9.88	19.78
		South-east (slope)	0.09	0.24	9.13	14.63
		West (slope)	0.11	0.27	4.52	17.31
	6–7 m	South-east (slope)	0.08	0.20	8.99	14.40
		West (slope)	0.08	0.17	3.94	8.65
West	2–3 m	Reef flat	0.15	0.23	8.86	10.91
		South-east (slope)	0.18	0.36	10.86	19.78
		West (slope)	0.18	0.74	8.90	10.98
	6–7 m	South-east (slope)	0.17	0.33	10.65	19.57
		West (slope)	0.16	0.72	8.89	11.61

$P < 0.001$, Table S19). In both seasons, shallow reef slope sites (2–3 m) experienced faster velocities on average than deeper sites (6–7 m) (Table S21). Curiously, the velocity did not vary significantly between sheltered and exposed sites. However, the exposed shallow reef did experience the greatest wave height and fastest velocity in both seasons (Fig. 4, Table 2).

3.2.2 Mobilisation across 3 d deployments

The relationship between velocity and rubble mobilisation across days was investigated for each season separately.

In the western monsoon, rubble was more likely to be transported and more likely to be flipped as the velocity increased, but only on day 1, resulting in an interaction between day and velocity (transport: Fig. 5a, $\chi^2 = 11.3$, $P = 0.004$; flipping: Fig. 5b, $\chi^2 = 7.416$, $P = 0.025$) (Tables S22, S23). For example, the probability of transport increased from 30 % to 60 %, moving from 0.1 to $0.4\,\mathrm{m\,s^{-1}}$ on day 1, but on day 2 these velocities both yielded only a 20 % chance of transport (Table S24). As for the likelihood of transport and flipping, rubble travelled slightly greater distances as velocity increased ($\chi^2 = 7.1$, $P = 0.008$) and trav-

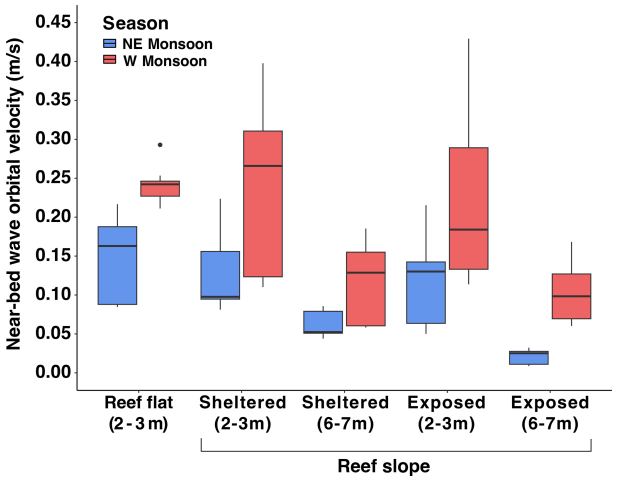

Figure 4. Boxplots for the nine (1 per day × 3 d × 3 sites) fastest near-bed wave orbital velocity values estimated for each habitat in each monsoonal observation period.

elled on average 1.6 cm more on day 1 than day 2 during the western monsoon (Fig. 5c, Tables S26, S27).

In the north-eastern monsoon, there was no relationship between velocity and rubble transport nor flipping, because the range of velocities captured in this season was comparatively narrower (Fig. 4). However, there was an effect of day on the probability of transport ($\chi^2 = 7.304$, $P = 0.026$, Table S28) and flipping in this season ($\chi^2 = 28.1$, $P < 0.001$, Table S29). At the mean velocity in the north-eastern monsoon ($0.1\,m\,s^{-1}$), the probability of flipping on day 1 was 13 % and fell on days 2 and 3 to only 6 % (Table S31). Rubble also travelled shorter distances on day 3 than day 1 (z ratio = 3.9, $P < 0.001$, Tables S32, S33).

3.2.3 Mobilisation thresholds

The mobilisation thresholds in the field were estimated using rubble movement data for day 1 only (as the most representative scenario to the flume trials; i.e. rubble pieces were newly deployed and not "settled") and using data from both seasons (to capture a wider range of velocities). The 50 % and 90 % mobilisation thresholds for transport (> 1 cm) in the field, averaged across all rubble sizes (4–23 cm), branchiness and substrate characteristics, were $0.30\,m\,s^{-1}$ (SE: 0.037) and $0.75\,m\,s^{-1}$ (SE: 0.146), respectively, on day 1 (Table S34). We note however that the 90 % threshold for transport is above the range of velocities measured in the field (Table S2) and should thus be considered cautiously compared to the 50 % threshold. We do not report the 50 % or 90 % thresholds for flipping in the field for the same reason.

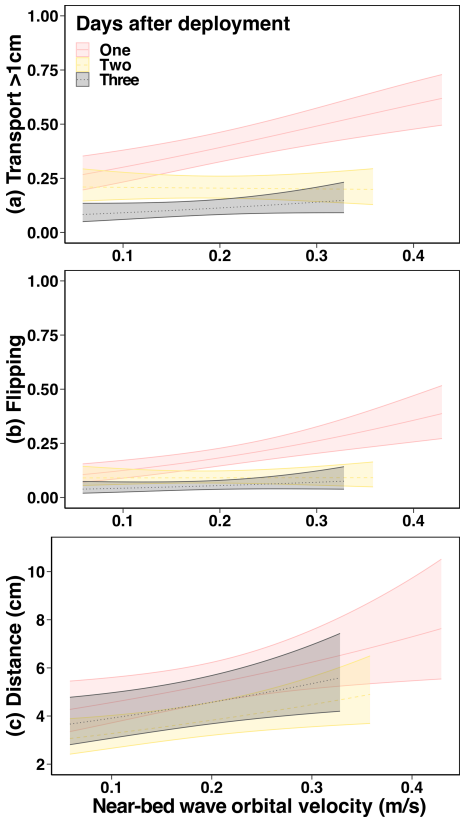

Figure 5. Relationship between near-bed wave orbital velocity ($m\,s^{-1}$) and **(a)** the probability of rubble transport (> 1 cm), **(b)** probability of flipping and **(c)** distance transported, on each day of the 3 d periods during the western monsoon (averaged across habitat).

3.2.4 Rubble and substrate effects on mobilisation

Probability of "transport" (walk/slide/flip)

To investigate the effects of rubble and substrate characteristics on the relationship between velocity and mobilisation in the field, data were also used from both seasons on day 1.

The probability of rubble transport (> 1 cm) on day 1 increased with velocity, but this relationship varied among rubble sizes ($\chi^2 = 10.039$, $P = 0.007$) (Fig. 6a, Table S35). At lower velocities, small, 4–8 cm rubble was transported more commonly than medium rubble, 9–15 cm, which moved more than large rubble, 16–23 cm. In the field, rubble of all sizes was equally likely to be transported at velocities $\geq 0.3\,m\,s^{-1}$ (Fig. 6a; Table S36), in contrast to the flume trials where smaller rubble always moved more than larger pieces across increasing velocities. Like the flume trials, rubble branchiness had a clear effect on rubble transport in the field, with unbranched rubble 1.7 times as likely to be transported as branched rubble (when averaged across velocity, substrate and size) (Table S37). The substrate type did

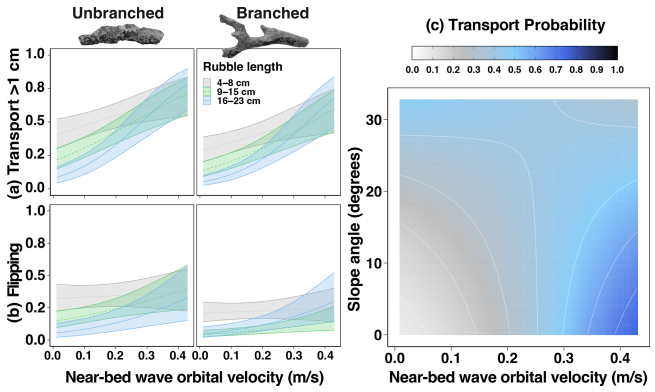

Figure 6. Relationship between near-bed wave orbital velocity ($m\,s^{-1}$) and the **(a)** probability of rubble transport (> 1 cm), **(b)** probability of flipping for each rubble size and branchiness type, and **(c)** how the slope angle and near-bed wave orbital velocity affect the probability of movement of rubble pieces.

not influence rubble transport in the field study ($\chi^2 = 0.4$, $P = 0.80$) (Table S35).

The relationship between velocity and transport changed with the steepness of the slope ($\chi^2 = 5.6$, $P < 0.001$) (Table S38). For flatter areas, rubble was more likely to be transported as velocity increased, whereas on steep slopes, the probability of transport did not increase by as much (Fig. 6c).

For example, at velocities of $0.1\,m\,s^{-1}$ and on very gentle slope angles of 3° (common on the reef flat), just 16 % (± 2.7 %, SE) of rubble would be transported, compared to 33 % (± 2.6 %) of rubble on 22° (steep) slopes, common at deep reef slope sites (Table S39). When water velocity increased to $0.4\,m\,s^{-1}$, rubble had a 69 % (± 7.8 %) chance and 48 % (± 1.1 %) chance of moving on very gentle and steep slopes, respectively (Fig. 6c). At velocities $\geq 0.2\,m\,s^{-1}$, there was no significant difference in the probability of transport across slope angles (Table S39).

Probability of flipping only

In the field, rubble was less likely to be flipped entirely than to be transported (Fig. 6b). As with the pattern observed for rubble transport, unbranched rubble flipped more commonly than branched rubble. However, unlike rubble transport, unbranched rubble only flipped more than branched rubble when it was small to medium, i.e. 4–15 cm in length ($\chi^2 = 8.3$, $P = 0.015$) (Tables S40, S41). Larger rubble of length 16–23 cm had a relatively low probability of flipping regardless of branchiness. Small (4–8 cm) rubble flipped more often than rubble sized from 9–23 cm (Table S42). However, as for transport, flipping became less dependent on rubble length as velocity increased, and all sizes were equally likely to flip at velocities $\geq 0.4\,m\,s^{-1}$ ($\chi^2 = 7.2$, $P = 0.03$) (Tables S40, S43).

Also, similarly to transport, the probability of flipping did not appear to vary with the substrate type ($\chi^2 = 4.9$, $P = 0.083$) (Table S40). Furthermore, while slope angle had some effect on the probability of transport, it did not affect the probability of rubble flipping in the field ($\chi^2 = 0.4$, $P = 0.536$) (Table S44).

Distance transported

The distance travelled by rubble increased with velocity ($\chi^2 = 12.3$, $P < 0.001$) but was not affected by rubble size or branchiness (Table S45). Substrate type, however, did affect the transport distance ($\chi^2 = 6.2$, $P = 0.046$). Just as smaller rubble moved more easily on sand in the wave flume, rubble travelled slightly further on sand (6.2 ± 0.8 cm averaged across velocities) than on rubble (4.7 ± 0.4 cm) over the course of 1 d (t ratio = −2.3, $P = 0.05$, Table S46).

As for transport probability, there was an interaction between velocity and slope for distance travelled ($\chi^2 = 26.2$, $P < 0.001$) (Table S47). At low velocities, rubble travelled greater distances as the steepness of the slope increased, likely aided by gravity. For example, on very gentle slopes (3°) rubble moved less distance (3 ± 0.2 cm, mean ± SE) than rubble on very strong (22°) slopes (5 ± 0.3 cm) at velocities of $0.1\,m\,s^{-1}$. Rubble travelled further as velocity increased on very gentle slopes (e.g. 22.9 ± 9.2 cm on 3° slopes at $0.4\,m\,s^{-1}$), but this pattern was not observed on steeper slopes at the same velocity (e.g. 3 ± 0.5 cm on 22° slopes) (Table S48).

4 Discussion

Here we characterised the physical parameters (i.e. near-bed wave orbital velocity, substrate type, reef slope angle) that influence rubble mobility in a flume and field setting across a range of rubble sizes and morphologies. As near-bed wave orbital velocity increased, rubble was more likely to rock, be transported and travel greater distances. Across flume and field environments, small and/or unbranched rubble pieces were generally mobilised at lower velocities than larger, branched rubble, while reef slope angle and substrate (sand or rubble) had more nuanced effects. Averaged across rubble and substrate types, the 50 % rocking threshold was slightly lower than the 50 % transport thresholds, which were almost identical between flume and day-1 field results. Interlocking and "settling" of rubble was a strong inhibitor of mobilisation, especially of transport. Interlocked rubble in the flume had only a 7 % chance of moving, and in the field, the likelihood of rubble mobilisation decreased over the course of the 3 d deployments. We hypothesise that rubble experienced "settling" or short-term stabilisation, whereby pieces were less likely to be transported on days 2 or 3 than day 1 at the same velocity. While the field results show rubble is capable of being mobilised during average wave conditions across the normal tidal cycle, if the rubble settling or interlocking effect is significant in an area, specific storm events

that cause higher velocities are likely to be more influential to mobilisation.

In the wave flume and in the field, 50 % of loose, cylindrical rubble ranging from 4–23 cm was transported at $0.3\,m\,s^{-1}$. Similar velocities to the reported thresholds have been observed on coral reefs globally, suggesting that rubble could be shifted under ambient conditions, depending on substrate, rubble typology and interlocking. Near-bed wave orbital velocities $> 0.3\,m\,s^{-1}$ have been reported on coral reefs in the Great Barrier Reef (Harris et al., 2015), Palmyra Atoll (Rogers et al., 2015; Monismith et al., 2015), Mo'orea (Monismith et al., 2013) and Puerto Rico (Viehman et al., 2018) and are likely common in nearshore and surf zone settings on reef slope, crests and flats. Wave and tide-induced current velocities above $0.3\,m\,s^{-1}$ are likely found on most coral reefs but not all reef environments (Kench, 1998a; Helmuth and Sebens, 1993; Sebens and Johnson, 1991). Threshold wave-orbital velocities in the present study are comparable to the modelled initiation of motion thresholds for rubble treated as simplified rectangular prisms with dimensions drawn from mean-sized rubble (length: ~ 3.3 cm, up to 10 cm) at a ship-grounding site on the south coast of Puerto Rico (Viehman et al., 2018). Reported wave-orbital thresholds were ~ 0.09–$0.2\,m\,s^{-1}$ for sliding and ~ 0.12–$0.34\,m\,s^{-1}$ for flipping, depending on rubble size and the degree of flow blocking by grouping. The thresholds reported in the present study differ in that they consider a wider range of rubble lengths and shapes, are observational as opposed to modelling based and are described in terms of probability rather than absolute initiation of motion.

The frequency at which rubble is transported (the transport return interval) will affect the length of stable periods or windows of recovery for coral recruitment and binding. Using hindcast wave modelling, Viehman et al. (2018) revealed the return interval for rubble sliding and overturning at their site in Puerto Rico was 7 and 12 d, respectively, with some, but not all, hindcast events aligning with tropical storms and cyclones (Viehman et al., 2018). Similarly, Cheroske et al. (2000) showed that rubble pieces tumbled on average about once every 15 d in Kāne'ohe Bay, Hawaii. However, the maximum flow speeds in the Kāne'ohe Bay study were relatively high, 0.6–$1.5\,m\,s^{-1}$ (Morgan and Kench, 2012), compared to wave-driven flows up to $0.43\,m\,s^{-1}$ at Vabbinfaru Reef. Owing to the protection afforded from storms and swell due to its location inside North Malé Atoll (Rasheed et al., 2021), we expect longer average return intervals on Vabbinfaru Reef. For example, islands < 5 km (Dhakandhoo) and 15 km (Hulhudhoo) from the western edge of nearby Southern Maalhosmadulu Atoll experience 60 % and 80 % reductions in wave height, respectively, compared to mean incident ocean swell (Kench et al., 2006; Young, 1999). Higher-energy movement events in the Maldives are likely driven more commonly by monsoonal wind patterns and clustered in the western monsoon. For example, during the north-eastern monsoon, a velocity of $0.3\,m\,s^{-1}$ (expected to transport 50 % of rubble pieces in the field) was never exceeded in 37 observed days, and in the western monsoon, it was exceeded on 4 of 32 d, at shallow sites only, with velocities exceeding $0.4\,m\,s^{-1}$ on only 1 d at an exposed shallow site in the western monsoon. Considering wind speeds and direction during observational periods for each monsoon typical of respective conditions over the past 33 years (Fig. S3), this indicates a transport return interval of ~ 8 d, but only at shallow sites during the western monsoon. Furthermore, we maintain that the return interval is likely to be much longer than this, considering that transport thresholds increase as rubble "settles" over time and as organisms such as sponges, bryozoans and crustose coralline algae bind rubble (Kenyon et al., 2023). However, while a window where conditions are too calm for transport is good for coral recruitment, binding between rubble pieces could yet be prevented by rocking motions, particularly for small, unbranched pieces (e.g. 50 % of loose, 4–8 cm unbranched rubble predicted to rock at $0.18\,m\,s^{-1}$ in the flume across substrates; Fig. 3a). Thus, we conservatively estimate that recovery windows for binding are likely to occur during the calmer north-eastern monsoon, when wave energy impacting the atoll is less and wave heights are smaller (Kench et al., 2006).

Curiously, at the same wave orbital velocity, the probability of rubble transport was lower in the north-eastern monsoon than in the western monsoon, suggesting there is greater complexity driving rubble transport than has been captured. For example, while the velocity across the day might be similar, sites in the western monsoon may have experienced a higher frequency of similar velocities throughout the day, providing more opportunities for mobilisation (supported by sites in the western monsoon having higher daily-average wave orbital velocities, as well as higher maximum velocities – Fig. S4). Alternatively, the greater hydrodynamic energy in the western monsoon may have primed the substrate to better facilitate transport. Even within the western monsoon, however, the probability of mobilisation decreased by ~ 10 % each day over the 3 d (velocity dependent). Rubble may have "settled" into more stable positions after being moved from the position in which they were placed by divers on day 1. Several rubble pieces shifted into crevices, particularly in shallow reef slope sites where hard carbonate and coral created a more structurally complex substrate than sandier, deeper slopes (Tania Kenyon, personal communication). On One Tree Island, Thornborough (2012) found branching rubble was regularly lodged under plate or boulder rubble or interlocked together into a rubble ridge within 6 d of the commencement of experiments. There, interlocked plate rubble also remains stable under energetic, tidally driven conditions (Thornborough, 2012). Presumably, higher velocities would be required to move rubble that has (a) settled deeper into the substrate by downward flow forcing or (b) wedged against a surface by lateral flow forcing. In the present study, some rubble still moved after settling on days 2 and 3, but manually interlocked rubble in the flume was very unlikely to be trans-

ported even at the maximum velocity of $0.42\,m\,s^{-1}$. Higher-energy, variable wave environments would likely foster more unstable rubble beds than lower-energy, constant wave environments, where rubble has time to settle. In these more energetic and/or variable settings and with smaller, simpler-shaped pieces, rubble may not settle and/or interlock routinely and could persist as an unstable bed for decades (Fox et al., 2019).

As expected, the threshold for rubble mobilisation varied according to rubble branchiness, in both controlled and reef environments. Generally, unbranched rubble was more likely to rock, walk, slide or flip than branched rubble. Branches can stabilise the rubble piece by digging into the sand or wedging against or beneath another rubble piece, thus explaining why living coral fragments with branching morphologies have increased post-breakage survival compared to those with non-branching morphologies (Tunnicliffe, 1981; Heyward and Collins, 1985; Smith and Hughes, 1999). Branched fragments and rubble would become lodged more easily in crevices or interlock together to form stable rubble beds, which can act as platforms for coral recruitment (Aronson and Precht, 1997). Size also affected the likelihood of mobilisation of rubble, reflecting studies on live fragment mobilisation and survival (Smith and Hughes, 1999; Hughes, 1999). Regardless of whether they had branches or not, small cylindrical rubble (particularly 4–8 cm) was more likely to be transported than larger pieces. However, size only influenced rubble transport in the field up to velocities of $0.3\,m\,s^{-1}$. Regardless, interventions might be considered at lower transport thresholds (e.g. 50 % of loose, 4–8 cm unbranched rubble predicted to move at $0.14\,m\,s^{-1}$ in the field; Fig. 6a) if a rubble bed is comprised predominantly of very small pieces, which is more commonly the case with anthropogenic disturbances such as ship groundings, human trampling and blast fishing (Kenyon et al., 2023). In Japan for example, rubble mounds formed seaward of coastal armouring were lower in weight, length and surface complexity than rubble from natural beds (Masucci et al., 2021).

We expected rubble to move more easily over sand, as shown previously (Heyward and Collins, 1985; Bruno, 1998; Bowden-Kerby, 2001; Prosper, 2005). However, substrate type had little effect on rubble mobilisation in the flume, except that small rubble was more likely to rock and be transported on sand than on rubble once velocities exceeded $0.2\,m\,s^{-1}$. In the field, although the distance travelled by rubble was slightly higher on sand than on rubble substrates, no effect of substrate on mobilisation probability was observed. This is potentially owing to the limited available sandy areas free of rubble on which to conduct trials as a consequence of the severe coral bleaching in the Maldives in 2016 (Perry and Morgan, 2017), leading to a mixed rubble–sand substrate. Greater distinction between substrates may have been observed in the flume if the first rubble substrate was comprised of larger-sized pieces more capable of "snagging" and interlocking the experimental pieces. The trials with the second rubble substrate demonstrated how interlocking provides a significant impediment to mobilisation. After an intense disturbance on a healthy reef, there is likely to be more rubble (multiple layers) and a greater proportion of rubble resting on other rubble, which – depending on branchiness and rubble size – could facilitate interlocking (Aronson and Precht, 1997). For smaller quantities of rubble, the rubble bed might be thinner (perhaps only one layer), and more rubble will be in contact with sand or hard carbonate substrate underneath, with less capacity for interlocking.

There were instances of rubble transport in the field even when the highest estimated velocity was $\sim 0.01\,m\,s^{-1}$. Several video observations of deployed rubble indicated no disturbance by fish and invertebrates, but this cannot be ruled out completely (Ormond and Edwards, 1987). Rubble movement on steeper sections of the slope was aided by gravity. In fact, all instances of movement at velocities $< 0.05\,m\,s^{-1}$ occurred in steep 6–7 m slope sites. Hughes (1999) found that fragments moved downslope in the absence of any major storms, most likely due to gravity-driven hillslope processes observed in marine and terrestrial systems (Salles et al., 2018). At lower velocities ($< 0.1\,m\,s^{-1}$) rubble was aided by gravity and was more likely to move and travel further on steeper slopes than flat and gentle slopes. Yet, as water velocity increased, rubble travelled shorter distances on steeper slopes. It is possible that higher velocities are indicative of waves with greater asymmetry that oppose gravitational transport and therefore maintain rubble at higher positions on the slopes, similar to the concept of equilibrium position of sediment on beach shorefaces over time (Ortiz and Ashton, 2016). While no significant relationship was detected between wave orbital velocity and direction of movement (upslope or downslope), a trend was observed. At shallow reef slope sites, which experienced higher velocities, ~ 19 % of rubble movements were upslope, compared to just ~ 3 % at deeper sites. Given the size of rubble, substantial upslope movement likely requires storm energy (Woodley et al., 1981b; Harmelin-Vivien and Laboute, 1986). Rubble might also travel further on flatter slopes at high velocities as a result of the association between slope and depth (i.e. flat and gentle slopes found primarily in reef flat and shallow sites and steep slopes primarily in deep sites). Reef flat and shallow slope sites experienced higher average velocities than deeper sites (Fig. S4) and thus experienced a higher frequency of velocities close to the maximum, providing more opportunities for mobilisation. Understanding the links between hydrodynamics and bathymetry of a disturbed reef is evidently important in determining its vulnerability to rubble mobilisation and recovery potential.

Two important factors to be considered in the context of the present study are the density or crowding of the rubble and the effect of rubble age on mobilisation thresholds. Following a disturbance, rubble will become increasingly distinct from recently killed coral in size, porosity, density and surficial encrustation, which will affect its hydrodynamic be-

haviour (Allen, 1990). Rubble is prone to further mechanical breakdown over time, due to incidental bioerosion by predators and grazers and direct bioerosion by borers (Scoffin, 1992; Perry and Hepbum, 2008), which may be exacerbated under certain environmental conditions, e.g. high nutrients and/or depth (Hallock, 1988; Pandolfi and Greenstein, 1997). Initially, rubble is expected to become less dense and more porous, as bioeroders and borers infiltrate the dead skeleton, although the time frames for these processes are largely unknown (but see Pari et al., 2002; Tribollet et al., 2002). The skeletal density of rubble used in the wave flume was $2.2 \pm 0.1\,\mathrm{g\,cm^{-3}}$ (mean $\pm$ SE) and on the reef was $1.9 \pm 0.04\,\mathrm{g\,cm^{-3}}$ (mean $\pm$ SE), which is similar to the mean coral skeletal density reported from a previous study at Vabbinfaru ($1.85\,\mathrm{g\,cm^{-3}}$) (Morgan and Kench, 2014b), suggesting that it had not been heavily bioeroded. Over time and with encrustation by coralline algae and in-filling of sediments into pores, cementation by magnesium calcite and aragonite could increase density (Scoffin, 1992), also affecting mobilisation thresholds. The bioerosional potential and subsequent mobilisation thresholds of rubble vary across different rubble morphologies and zones. Bioerosional processes proceed more readily in deeper, lower-energy environments and in more dense, massive morphologies compared to branching rubble, likely due to their higher residence times in active bioerosion zones (Pandolfi and Greenstein, 1997; Greenstein and Pandolfi, 2003; Perry and Hepbum, 2008). The density of branching coral rubble might remain higher than massive coral rubble, resulting in higher velocity thresholds (Pandolfi and Greenstein, 1997). Yet, branching morphologies are also more prone to breakage, leading to smaller pieces and subsequently more movement.

Mobilisation thresholds will also be affected by how many rubble pieces are in a rubble bed. Notably, thresholds are likely to be lower for individual pieces, used in the current study, as they are exposed to flow on all sides. Densely packed rubble is likely to be more stable than individual pieces, even without interlocking, due to the protection afforded by surrounding rubble. Similar considerations are made when assessing transport of boulders surrounded by rock on the lee side of flow, which have a higher threshold of motion than free (not surrounded) boulders (Nott, 2003; Nandasena et al., 2011). In modelling the mobilisation thresholds of oblong-shaped rubble exposed to flow, Viehman (2018) applied a blocking factor to vary the amount of rubble area exposed to flow because of varying degrees of crowding (Storlazzi et al., 2005). Surprisingly, this factor resulted in only very slight variations in the sliding and overturning thresholds. Tajima and Seto (2017) reported that most pieces in coral gravel beds shifted at $0.25–0.5\,\mathrm{m\,s^{-1}}$, a comparable threshold to that reported for rubble pieces here, yet pieces in these gravel beds were small, only up to 2 cm. Mobilisation of beds of larger-sized rubble common on coral reefs should be investigated in further trials in a controlled wave flume environment. Individual pieces in moveable, natural rubble beds could also be tagged and tracked over longer periods to further understand mobilisation in a bed.

Implications for management

The scale of reef degradation and subsequent intervention methods is vast, putting pressure on reef restoration budgets. While operationalising the implementation of reef restoration at scale is investigated (Saunders et al., 2020), tools that allow managers to prioritise reefs that are particularly vulnerable to rubble mobilisation, and thus longer natural recovery times, are essential (Kenyon et al., 2023). The results of this study provide information toward improved management of damaged reefs with high rubble cover. Broadly, rubble stabilisation interventions might be considered at lower mobilisation thresholds if a rubble bed is composed mostly of loose (not interlocked), small pieces, particularly with low morphological complexity, which is more commonly the case with anthropogenic disturbances such as ship groundings, human trampling, coastal armouring and blast fishing (Masucci et al., 2021; Kenyon et al., 2023). Importantly, groove sites can also be characterised by these rubble types (Wolfe et al., 2023) but should not be considered for interventions because they are geomorphological features with hydrodynamic conditions commonly driving rubble entrainment and deposition (Shannon et al., 2013; Duce et al., 2022). More comprehensively, the mobilisation estimates reported here can be used in modelling frameworks that predict the frequency of everyday rubble mobilisation in a certain location, based on a modelled time series of wave climate estimates, such as the everyday wave conditions model developed for the Great Barrier Reef (Roelfsema et al., 2020). Reefs or areas of reefs at higher risk of frequent rubble mobilisation can be prioritised for rubble stabilisation interventions following disturbances, with predictions being improved through consideration of the mobilisation processes discussed, e.g. settling and interlocking over time; bathymetry (e.g. slope, geomorphology); rubble quantity, size and morphology (driven by disturbance, surrounding coral cover and diversity); water quality; and bioerosion.

Code and data availability. Datasets and code are available at https://doi.org/10.5281/zenodo.10032448 (Kenyon, 2023).

Supplement. The supplement related to this article is available online at: https://doi.org/10.5194/bg-20-4339-2023-supplement.

Author contributions. TMK, DH, CD and PJM conceived field experiments. TMK, TB, DC and PJM conceived flume experiments. TMK conducted flume and fieldwork, processed and analysed data, and wrote the text. DH, TB, DC, CD, GW, SPN and PJM contributed and edited the text. DH, CD, GW, SPN and PJM provided supervision.

Competing interests. The contact author has declared that none of the authors has any competing interests.

Acknowledgements. This study was conducted in collaboration with the Banyan Tree Marine Laboratory. In-kind contributions were received from Banyan Tree Vabbinfaru and Angsana Ihuru, including the Dive Centre, headed by Mujuthaba Ali. We wish to acknowledge Mohamed Arzan, Zim Athif, Amal Charles Everitt, Samantha Gallimore, Danielle Robinson, Crystle Wee, Toby Mitchell, Ahmed Tholal, Ali Nasheed, Jason Van Der Gevel, Stewart Matthews, Ananth Wuppukondur, Matthew Florence and Nick Brilli for assistance in the field and laboratory. Limited impact accreditation no. UQ005/2016 was used for the collection of rubble used in the flume.

Financial support. This study was funded in part by a PADI Foundation Grant and GBRMPA Science for Management Award to Tania M. Kenyon and ARC grants to Peter J. Mumby. Support was also provided by an Australian Government Research Training Program (RTP) Scholarship (stipend) and from the Australian Government's Reef Restoration and Adaptation Program (RRAP).

Disclaimer. Publisher's note: Copernicus Publications remains neutral with regard to jurisdictional claims in published maps and institutional affiliations.

Review statement. This paper was edited by Andrew Thurber and reviewed by two anonymous referees.

References

Allen, J. R. L.: Transport – hydrodynamics: shells, in: Palaeobiology: a synthesis, edited by: Briggs, D. E. G. and Crowther, P. R., Blackwell Scientific Publications, Oxford, 227–230, ISBN 063203118, 1990.

Alvarez-Filip, L., Dulvy, N. K., Gill, J. A., Côté, I. M., and Watkinson, A. R.: Flattening of Caribbean coral reefs: Region-wide declines in architectural complexity, Proc. R. Soc. B, 276, 3019–3025, https://doi.org/10.1098/rspb.2009.0339, 2009.

Aronson, R. B. and Precht, W. F.: Stasis, Biological Disturbance, and Community Structure of a Holocene Coral Reef, Palepbiology, 23, 326–346, https://doi.org/10.1017/S0094837300019710, 1997.

Baldock, T. E., Golshani, A., Callaghan, D. P., Saunders, M. I., and Mumby, P. J.: Impact of sea-level rise and coral mortality on the wave dynamics and wave forces on barrier reefs, Mar. Pollut. Bull., 83, 155–164, https://doi.org/10.1016/j.marpolbul.2014.03.058, 2014a.

Baldock, T. E., Karampour, H., Sleep, R., Vyltla, A., Albermani, F., Golshani, A., Callaghan, D. P., Roff, G., and Mumby, P. J.: Resilience of branching and massive corals to wave loading under sea level rise – A coupled computational fluid dynamics-structural analysis, Mar. Pollut. Bull., 86, 91–101, https://doi.org/10.1016/j.marpolbul.2014.07.038, 2014b.

Baldock, T. E., Birrien, F., Atkinson, A., Shimamoto, T., Wu, S., Callaghan, D. P., and Nielsen, P.: Morphological hysteresis in the evolution of beach profiles under sequences of wave climates – Part 1; Observations, Coast. Eng., 128, 92–105, https://doi.org/10.1016/j.coastaleng.2017.08.005, 2017.

Bartoń, K.: MuMIn: Multi-Model Inference, https://cran.r-project.org/package=MuMIn (last access: 23 October 2023), 2020.

Beetham, E. P. and Kench, P. S.: Wave energy gradients and shoreline change on Vabbinfaru platform, Maldives, Geomorphology, 209, 98–110, 2014.

Blair, T. C. and McPherson, J. G.: Grain-size and textural classification of coarse sedimentary particles, J. Sediment. Res., 69, 6–19, https://doi.org/10.2110/jsr.69.6, 1999.

Blanchon, P. and Jones, B.: Hurricane control on shelf-edge-reef architecture around Grand Cayman, Sedimentology, 44, 479–506, https://doi.org/10.1046/j.1365-3091.1997.d01-32.x, 1997.

Blanchon, P., Jones, B., and Kalbfleisch, W.: Anatomy of a fringing reef around Grand Cayman: storm rubble, not coral framework, J. Sediment. Res., 67, 1–16, https://doi.org/10.1306/D42684D7-2B26-11D7-8648000102C1865D, 1997.

Bowden-Kerby, A.: Low-tech coral reef restoration methods modeled after natural fragmentation processes, Bull. Mar. Sci., 69, 915–931, 2001.

Brooks, M. E., Kristensen, K., van Benthen, K. J., Magnusson, A., Berg, C. W., Nielsen, A., Skaug, H. J., Maechler, M., and Bolker, B. M.: glmmTMB Balances Speed and Flexibility Among Packages for Zero-inflated Generalized Linear Mixed Modeling, R J., 9, 378–400, 2017.

Brown, B. E. and Dunne, D. P.: The environmental impact of coral mining on coral reefs in the Maldives, Environ. Conserv., 15, 159–166, 1988.

Bruno, J. F.: Fragmentation in Madracis mirabilis (Duchassaing and Michelotti): How common is size-specific fragment survivorship in corals?, J. Exp. Mar. Bio. Ecol., 230, 169–181, https://doi.org/10.1016/S0022-0981(98)00080-X, 1998.

Cheroske, A. G., Williams, S. L., and Carpenter, R. C.: Effects of physical and biological disturbances on algal turfs in Kaneohe Bay, Hawaii, J. Exp. Mar. Bio. Ecol., 248, 1–34, 2000.

Chong-Seng, K. M., Graham, N. A. J., and Pratchett, M. S.: Bottlenecks to coral recovery in the Seychelles, Coral Reefs, 33, 449–461, https://doi.org/10.1007/s00338-014-1137-2, 2014.

Clark, S. and Edwards, A. J.: Coral transplantation as an aid to reef rehabilitation: evaluation of a case study in the Maldive Islands, Coral. Reefs, 14, 201–213, 1995.

Clark, T. R., Roff, G., Zhao, J. xin, Feng, Y. xing, Done, T. J., McCook, L. J., and Pandolfi, J. M.: U-Th dating reveals regional-scale decline of branching Acropora corals on the Great Barrier Reef over the past century, P. Natl. Acad. Sci. USA, 114, 10350–10355, https://doi.org/10.1073/pnas.1705351114, 2017.

Davies, P. J.: Reef growth, in: Perspectives on coral reefs, edited by: Barnes, D. J., Clouston, Manuka, 69–106, https://www.abebooks.com/first-edition/Perspectives-Coral-Reefs-Barnes-D-J/81606367/bd (last access: 23 October 2023) 1983.

Dollar, S. and Tribble, G. W.: Recurrent storm disturbance and recovery: a long-term study of coral communities in Hawaii, Coral

Reefs, 12, 223–233, https://doi.org/10.1016/B978-0-12-811963-1.00001-9, 1993.

Duce, S., Vila-Concejo, A., McCarroll, R. J., Yiu, B., Perris, L. A., and Webster, J. M.: Field measurements show rough fore reefs with spurs and grooves can dissipate more wave energy than the reef crest, Geomorphology, 413, 108365, https://doi.org/10.1016/j.geomorph.2022.108365, 2022.

Etienne, S. and Paris, R.: Boulder accumulations related to storms on the south coast of the Reykjanes Peninsula (Iceland), Geomorphology, 114, 55–70, https://doi.org/10.1016/j.geomorph.2009.02.008, 2010.

Ferrario, F., Beck, M. W., Storlazzi, C. D., Micheli, F., Shepard, C. C., and Airoldi, L.: The effectiveness of coral reefs for coastal hazard risk reduction and adaptation, Nat. Commun., 5, 1–9, https://doi.org/10.1038/ncomms4794, 2014.

Fong, P. and Lirman, D.: Hurricanes Cause Population Expansion of the Branching Coral Acropora palmata (Scleractinia): Wound Healing and Growth Patterns of Asexual Recruits, Mar. Ecol., 16, 317–335, https://doi.org/10.1111/j.1439-0485.1995.tb00415.x, 1995.

Fox, H. E. and Caldwell, R. L.: Recovery from blast fishing on coral reefs: A tale of two scales, Ecol. Appl., 16, 1631–1635, https://doi.org/10.1890/1051-0761(2006)016[1631:Rfbfoc]2.0.Co;2, 2006.

Fox, H. E., Harris, J. L., Darling, E. S., Ahmadia, G. N., and Razak, T. B.: Rebuilding coral reefs: success (and failure) 16 years after low-cost, low-tech restoration, Restor. Ecol., 27, 862–869, https://doi.org/10.1111/rec.12935, 2019.

Gittings, S. R., Bright, T. J., and Hagman, D. K.: The M/V Wellwood and other large vessel groundings: coral reef damage and recovery, in: Proc Colloquium on Global Aspects of Coral Reefs: Health, Hazards and History, edited by: Ginsburg, R. N., Rosenstiel School of Marine and Atmospheric Science, Miami, 174–180, https://scholar.google.com/scholar_lookup?title=Proc+Colloquium+on+Global+Aspects+of+Coral+Reefs:+Health,+Hazards+and+History&author=SR+Gittings&author=TJ+Bright&author=DK+Hagman&author=RN+Ginsburg&publication_year=1994& (last access: 23 October 2023) 1994.

Graham, N. A. J., Wilson, S. K., Jennings, S., Polunin, N. V. C., Bijoux, J. P., and Robinson, J.: Dynamic fragility of oceanic coral reef ecosystems, P. Natl. Acad. Sci. USA, 103, 8425–8429, 2006.

Greenstein, B. J. and Pandolfi, J. M.: Taphonomic alteration of reef corals: Effects of reef environment and coral growth form II: The Florida Keys, Palaios, 18, 495–509, 2003.

Guihen, D., White, M., and Lundalv, T.: Boundary layer flow dynamics at a cold-water coral reef, J. Sea Res., 78, 36–44, https://doi.org/10.1016/j.seares.2012.12.007, 2013.

Hallock, P.: The role of nutrient availability in bioerosion: Consequences to carbonate buildups, Palaeogeogr. Palaeocl., 63, 275–291, https://doi.org/10.1016/0031-0182(88)90100-9, 1988.

Hardison, B. S. and Layzer, J. B.: Relations between complex hydraulics and the localized distribution of mussels in three regulated rivers, River Res. Appl., 17, 77–84, https://doi.org/10.1002/1099-1646(200101/02)17:1<77::aid-rrr604>3.0.co;2-s, 2001.

Harmelin-Vivien, M. L. and Laboute, P.: Catastrophic impact of hurricanes on atoll outer reef slopes in the Tuamotu (French Polynesia), Coral Reefs, 5, 55–62, https://doi.org/10.1007/BF00270353, 1986.

Harris, D. L., Vila-Concejo, A., Webster, J. M., and Power, H. E.: Spatial variations in wave transformation and sediment entrainment on a coral reef sand apron, Mar. Geol., 363, 220–229, https://doi.org/10.1016/j.margeo.2015.02.010, 2015.

Harris, D. L., Rovere, A., Casella, E., Power, H., Canavesio, R., Collin, A., Pomeroy, A., Webster, J. M., and Parravicini, V.: Coral reef structural complexity provides important coastal protection from waves under rising sea levels, Sci. Adv., 4, 1–8, https://doi.org/10.1126/sciadv.aao4350, 2018a.

Harris, D. L., Power, H. E., Kinsela, M. A., Webster, J. M., and Vila-Concejo, A.: Variability of depth-limited waves in coral reef surf zones, Estuar. Coast. Shelf Sci., 211, 36–44, https://doi.org/10.1016/j.ecss.2018.06.010, 2018b.

Hawkins, J. P. and Roberts, C. M.: Effects of Recreational Scuba Diving on Coral Reefs: Trampling on Reef-Flat Communities, J. Appl. Ecol., 30, 25–30, 1993.

Helmuth, B. and Sebens, K.: The influence of colony morphology and orientation to flow on particle capture by the scleractinian coral Agaricia agaricites (Linnaeus), J. Exp. Mar. Bio. Ecol., 165, 251–278, https://doi.org/10.1016/0022-0981(93)90109-2, 1993.

Heyward, A. J. and Collins, J. D.: Fragmentation in Montiporaramosa: the genet and ramet concept applied to a reef coral, Coral Reefs, 4, 35–40, 1985.

Highsmith, R. C.: Reproduction by fragmentation in corals, Mar. Ecol. Prog. Ser., 7, 207–226, https://doi.org/10.3354/meps007207, 1982.

Highsmith, R. C., Riggs, A. C., and D'Antonio, C. M.: Survival of Hurricane-Generated Coral Fragments and a Disturbance Model of Reef Calcification/Growth Rates, Oecologia, 46, 322–329, 1980.

Hoegh-Guldberg, O.: Climate change, coral bleaching and the future of the world's coral reefs, Mar. Freshw. Res., 50, 839–866, 1999.

Hoegh-Guldberg, O., Mumby, P. J., Hooten, A. J., Steneck, R. S., Greenfield, P., Gomez, E., Harvell, C. D., Sale, P. F., Edwards, A. J., Caldeira, K., Knowlton, N., Eakin, C. M., Iglesias-Prieto, Muthiga, N., Bradbury, R. H., Dubi, A., and Hatziolos, M. E.: Coral reefs under rapid climate change and ocean acidification, Science, 318, 1737–1742, 2007.

Hubbard, D. K.: Hurricane-induced sediment transport in open-shelf tropical systems – an example from St.Croix, U.S. Virgin Islands, J. Sediment. Res., 62, 946–960, 1992.

Hughes, M. G. and Moseley, A. S.: Hydrokinematic regions within the swash zone, Cont. Shelf Res., 27, 2000–2013, https://doi.org/10.1016/j.csr.2007.04.005, 2007.

Hughes, T. P.: Off-reef transport of coral fragments at Lizard Island, Australia, Mar. Geol., 157, 1–6, 1999.

Hughes, T. P., Kerry, J. T., Baird, A. H., Connolly, S. R., Dietzel, A., Eakin, C. M., Heron, S. F., Hoey, A. S., Hoogenboom, M. O., Liu, G., McWilliam, M. J., Pears, R. J., Pratchett, M. S., Skirving, W. J., Stella, J. S., and Torda, G.: Global warming transforms coral reef assemblages, Nature, 556, 492–496, https://doi.org/10.1038/s41586-018-0041-2, 2018.

Imamura, F., Goto, K., and Ohkubo, S.: A numerical model for the transport of a boulder by tsunami, J. Geophys. Res.-Ocean., 113, 1–12, https://doi.org/10.1029/2007JC004170, 2008.

Kain, C. L., Gomez, C., and Moghaddam, A. E.: Comment on "Reassessment of hydrodynamic equations: Minimum flow velocity to initiate boulder transport by high energy events

(storms, tsunamis)" by N. A. K. Nandasena, R. Paris and N. Tanaka, Mar. Geol., 281, 70–84, Mar. Geol., 319–322, 75–76, https://doi.org/10.1016/j.margeo.2011.08.008, 2012.

Kay, A. M. and Liddle, M. J.: Impact of human trampling in different zones of a coral reef flat, Environ. Manage., 13, 509–520, https://doi.org/10.1007/BF01867685, 1989.

Keen, T. R., Bentley, S. J., Chad Vaughan, W., and Blain, C. A.: The generation and preservation of multiple hurricane beds in the northern Gulf of Mexico, Mar. Geol., 210, 79–105, https://doi.org/10.1016/j.margeo.2004.05.022, 2004.

Kench, P. S.: A currents of removal approach for interpreting carbonate sedimentary processes, Mar. Geol., 145, 197–223, https://doi.org/10.1016/S0025-3227(97)00101-1, 1998a.

Kench, P. S.: Physical controls on development of lagoon sand deposits and lagoon infilling in an Indian Ocean atoll, J. Coast. Res., 14, 1014–1024, 1998b.

Kench, P. S., Brander, R. W., Parnell, K. E., and McLean, R. F.: Wave energy gradients across a Maldivian atoll: Implications for island geomorphology, Geomorphology, 81, 1–17, https://doi.org/10.1016/j.geomorph.2006.03.003, 2006.

Kench, P. S., Brander, R. W., Parnell, K. E., and O'Callaghan, J. M.: Seasonal variations in wave characteristics around a coral reef island, South Maalhosmadulu atoll, Maldives, Mar. Geol., 262, 116–129, https://doi.org/10.1016/j.margeo.2009.03.018, 2009.

Kenyon, T. M.: TMKenyon/rubblemobthresholds: Kenyon et al. 2023 Biogeosciences Publication (Version v1), Zenodo [code and data set], https://doi.org/10.5281/zenodo.10032448, 2023.

Kenyon, T. M., Doropoulos, C., Dove, S., Webb, G., Newman, S., Sim Wei Hung, C., Arzan, M., and Mumby, P. J.: The effects of rubble mobilisation on coral fragment survival, partial mortality and growth, J. Exp. Mar. Bio. Ecol., 533, 151467, https://doi.org/10.1016/j.jembe.2020.151467, 2020.

Kenyon, T. M., Doropoulos, C., Wolfe, K., Webb, G. E., Dove, S., Harris, D., and Mumby, P. J.: Coral rubble dynamics in the Anthropocene and implications for reef recovery, Limnol. Oceanogr., 68, 110–147, https://doi.org/10.1002/lno.12254, 2023.

Knutson, T. R., McBride, J. L., Chan, J., Emanuel, K., Holland, G., Landsea, C., Held, I., Kossin, J. P., Srivastava, A. K., and Sugi, M.: Tropical cyclones and climate change, Nat. Geosci., 3, 157–163, https://doi.org/10.1038/ngeo779, 2010.

Komar, P. D. and Miller, M. C.: The threshold of sediment movement under oscillatory water waves, J. Sediment. Petrol., 43, 1101–1110, 1973.

Lasagna, R., Albertelli, G., Giovannetti, E., Grondona, M., Milani, A., Morri, C., and Bianchi, C. N.: Status of Maldivian reefs eight years after the 1998 coral mass mortality, Chem. Ecol., 24, 67–72, 2008.

Lenth, R. V.: emmeans: Estimated Marginal Means, aka Least-Squares Means, R package version 1.8.7, https://CRAN.R-project.org/package=emmeans (last access: 23 October 2023), 2020.

Lewis, J. B.: Evidence from aerial photography of structural loss of coral reefs at Barbados, West Indies, Coral Reefs, 21, 49–56, https://doi.org/10.1007/s00338-001-0198-1, 2002.

Liu, E. T., Zhao, J. X., Feng, Y. X., Leonard, N. D., Clark, T. R., and Roff, G.: U-Th age distribution of coral fragments from multiple rubble ridges within the Frankland Islands, Great Barrier Reef: Implications for past storminess history, Quaternary Sci. Rev., 143, 51–68, https://doi.org/10.1016/j.quascirev.2016.05.006, 2016.

Luckhurst, B. E. and Luckhurst, K.: Analysis of the influence of substrate variables on coral reef fish communities, Mar. Biol., 49, 317–323, https://doi.org/10.1007/BF00455026, 1978.

Masucci, G. D., Biondi, P., and Reimer, J. D.: A Comparison of Size, Shape, and Fractal Diversity Between Coral Rubble Sampled From Natural and Artificial Coastlines Around Okinawa Island, Japan, Front. Mar. Sci., 8, 1–8, https://doi.org/10.3389/fmars.2021.703698, 2021.

Meehl, G. A., Tebaldi, C., Teng, H., and Peterson, T. C.: Current and future US weather extremes and El Niño, Geophys. Res. Lett., 34, 1–6, https://doi.org/10.1029/2007GL031027, 2007.

Monismith, S. G., Herdman, L. M. M., Ahmerkamp, S., and Hench, J. L.: Wave transformation and wave-driven flow across a steep coral reef, J. Phys. Oceanogr., 43, 1356–1379, https://doi.org/10.1175/JPO-D-12-0164.1, 2013.

Monismith, S. G., Rogers, J. S., Koweek, D., and Dunbar, R. B.: Frictional wave dissipation on a remarkably rough reef, Geophys. Res. Lett., 42, 4063–4071, https://doi.org/10.1002/2015GL063804, 2015.

Montaggioni, L. F.: History of Indo-Pacific coral reef systems since the last glaciation: Development patterns and controlling factors, Earth-Sci. Rev., 71, 1–75, https://doi.org/10.1016/j.earscirev.2005.01.002, 2005.

Morgan, K. and Kench, P.: Export of reef-derived sediments on Vabbinfaru reef platform, Maldives, in: Proc. 12th Int. Coral Reef Symp., 9–13 July 2012, Cairns, https://www.icrs2012.com/proceedings/manuscripts/ICRS2012_1A_3.pdf (last access: 23 October 2023), 2012.

Morgan, K. M. and Kench, P. S.: A detrital sediment budget of a Maldivian reef platform, Geomorphology, 222, 122–131, https://doi.org/10.1016/j.geomorph.2014.02.013, 2014a.

Morgan, K. M. and Kench, P. S.: A detrital sediment budget of a Maldivian reef platform, Geomorphology, 222, 122–131, https://doi.org/10.1016/j.geomorph.2014.02.013, 2014b.

Nandasena, N. A. K., Paris, R., and Tanaka, N.: Reassessment of hydrodynamic equations: Minimum flow velocity to initiate boulder transport by high energy events (storms, tsunamis), Mar. Geol., 281, 70–84, https://doi.org/10.1016/j.margeo.2011.02.005, 2011.

Nielsen, P. and Callaghan, D. P.: Shear stress and sediment transport calculations for sheet flow under waves, Coast. Eng., 47, 347–354, https://doi.org/10.1016/S0378-3839(02)00141-2, 2003.

Nott, J.: Extremely high-energy wave deposits inside the Great Barrier Reef, Australia: Determining the cause-tsunami or tropical cyclone, Mar. Geol., 141, 193–207, https://doi.org/10.1016/S0025-3227(97)00063-7, 1997.

Nott, J.: Waves, coastal boulder deposits and the importance of the pre-transport setting, Earth Planet. Sc. Lett., 210, 269–276, https://doi.org/10.1016/S0012-821X(03)00104-3, 2003.

Ormond, R. F. G. and Edwards, A.: Red Sea Fishes, in: Red Sea, edited by: Edwards, A. J. and Head, S. M., Pergamon Press, Oxford, UK, 252–287, 1987.

Ortiz, A. C. and Ashton, A. D.: Exploring shoreface dynamics and a mechanistic explanation for a morphodynamic depth of closure, J. Geophys. Res.-Earth, 121, 442–464, https://doi.org/10.1002/2015JF003699, 2016.

Pandolfi, J. M. and Greenstein, B. J.: Taphonomic alteration of reef corals: Effects of reef environment and coral growth form, I. The Great Barrier Reef, Palaios, 12, 27–42, https://doi.org/10.2307/3515292, 1997.

Pari, N., Peyrot-Clausade, M., and Hutchings, P. A.: Bioerosion of experimental substrates on high islands and atoll lagoons (French Polynesia) during 5 years of exposure, J. Exp. Mar. Bio. Ecol., 276, 109–127, https://doi.org/10.1016/S0022-0981(02)00243-5, 2002.

Perry, C. T. and Morgan, K. M.: Post-bleaching coral community change on southern Maldivian reefs: is there potential for rapid recovery?, Coral Reefs, 36, 1189–1194, https://doi.org/10.1007/s00338-017-1610-9, 2017.

Pinheiro, J., Bates, D., DebRoy, S., Sarkar, D., and R Core Team: nlme: Linear and Nonlinear Mixed Effects Models, R package version 3.1-162, https://cran.r-project.org/package=nlme (last access: 23 October 2023), 2019.

Prosper, A. L. O.: Population Dynamics of Hurricane-Generated Fragments of Elkhorn Coral Acropora palmata, Lamarck, 1816, PhD Thesis, University of Puerto Rico, 74 pp., https://www.aoml.noaa.gov/general/lib/CREWS/Cleo/PuertoRico/prpdfs/ortiz-population.pdf (last access: 23 October 2023), 2005.

R Core Team: R: A Language and Environment for Statistical Computing, R Foundation for Statistical Computing, Vienna, Austria, https://www.R-project.org/ (last access: 23 October 2023), 2020.

Rasheed, S., Warder, S. C., Plancherel, Y., and Piggott, M. D.: Response of tidal flow regime and sediment transport in North Male' Atoll, Maldives to coastal modification and sea level rise, Ocean Sci., 17, 319–334, https://doi.org/10.5194/os-17-319-2021, 2021.

Rasser, M. W. and Riegl, B.: Holocene coral reef rubble and its binding agents, Coral Reefs, 21, 57–72, https://doi.org/10.1007/s00338-001-0206-5, 2002.

Roelfsema, C. M., Kovacs, E. M., Ortiz, J. C., Callaghan, D. P., Hock, K., Mongin, M., Johansen, K., Mumby, P. J., Wettle, M., Ronan, M., Lundgren, P., Kennedy, E. V., and Phinn, S. R.: Habitat maps to enhance monitoring and management of the Great Barrier Reef, Coral Reefs, 39, 1039–1054, https://doi.org/10.1007/s00338-020-01929-3, 2020.

Rogers, A., Blanchard, J. L., and Mumby, P. J.: Fisheries productivity under progressive coral reef degradation, J. Appl. Ecol., 55, 1041–1049, https://doi.org/10.1111/1365-2664.13051, 2018.

Rogers, J., Monismith, S. G., Koweek, D. A., and Dunbar, R. B.: Wave dynamics of a Pacific Atoll with high frictional effects, J. Geophys. Res.-Ocean., 121, 476–501, https://doi.org/10.1002/2015JC011170.Received, 2015.

Salles, T., Ding, X., and Brocard, G.: pyBadlands: A framework to simulate sediment transport, landscape dynamics and basin stratigraphic evolution through space and time, PLoS One, 13, 1–24, https://doi.org/10.1371/journal.pone.0195557, 2018.

Saunders, M. I., Doropoulos, C., Bayraktarov, E., Babcock, R. C., Gorman, D., Eger, A. M., Vozzo, M. L., Gillies, C. L., Vanderklift, M. A., Steven, A. D. L., Bustamante, R. H., and Silliman, B. R.: Bright Spots in Coastal Marine Ecosystem Restoration, Curr. Biol., 30, R1500–R1510, https://doi.org/10.1016/j.cub.2020.10.056, 2020.

Scoffin, T. P.: Taphonomy of coral reefs: a review, Coral Reefs, 11, 57–77, 1992.

Scoffin, T. P.: The geological effects of hurricanes on coral reefs and the interpretation of storm deposits, Coral Reefs, 12, 203– 221, 1993.

Scoffin, T. P. and McLean, R. F.: Exposed limestones of the northern province of the Great Barrier Reef, Phil. Trans. R. Soc. Lond. A, 291, 119–138, 1978.

Sebens, K. P. and Johnson, A. S.: Effects of water movement on prey capture and distribution of reef corals, Hydrobiologia, 216, 247–248, 1991.

Shannon, A. M., Power, H. E., Webster, J. M., and Vila-Concejo, A.: Evolution of Coral Rubble Deposits on a Reef Platform as Detected by Remote Sensing, Remote Sens., 5, 1–18, https://doi.org/10.3390/rs5010001, 2013.

Smith, L. D. and Hughes, T. P.: An experimental assessment of survival, re-attachment and fecundity of coral fragments, J. Exp. Mar. Bio. Ecol., 235, 147–164, 1999.

Soulsby, R. L.: Sand Transport in Oscillatory Flow: Simplified calculation of wave orbital velocities, HR Wallingford Ltd, Oxfordshire, UK, https://eprints.hrwallingford.com/588/1/TR155.pdf (last access: 23 October 2023), 2006.

Sousa, W. P.: Experimental Investigations of Disturbance and Ecological Succession in a Rocky Intertidal Algal Community, Ecol. Monogr., 49, 227–254, 1979.

Storlazzi, C. D., Brown, E. K., Field, M. E., Rodgers, K., and Jokiel, P. L.: A model for wave control on coral breakage and species distribution in the Hawaiian Islands, Coral Reefs, 24, 43–55, https://doi.org/10.1007/s00338-004-0430-x, 2005.

Suren, A. M. and Duncan, M. J.: Rolling stones and mosses: Effect of substrate stability on bryophyte communities in streams, J. North Am. Benthol. Soc., 18, 457–467, https://doi.org/10.2307/1468378, 1999.

Tajima, Y. and Seto, S.: Laboratory Study On Transport Of Coral Gravals Under Forward-Leaning Nearshore Waves, Coast. Dynam., 164, 966–975, 2017.

Thornborough, K. J.: Rubble-dominated reef flat processes and development: evidence from One Tree Reef, Southern Great Barrier Reef, PhD Thesis, The University of Sydney, 121 pp., https://doi.org/10.13140/RG.2.1.2556.0487, 2012.

Townsend, C. R., Scarsbrook, M. R., and Dolédec, S.: The intermediate disturbance hypothesis, refugia, and biodiversity in streams, Limnol. Oceanogr., 42, 938–949, https://doi.org/10.4319/lo.1997.42.5.0938, 1997.

Tribollet, A., Decherf, G., Hutchings, P. A., and Peyrot-Clausade, M.: Large-scale spatial variability in bioerosion of experimental coral substrates on the Great Barrier Reef (Australia): Importance of microborers, Coral Reefs, 21, 424–432, https://doi.org/10.1007/s00338-002-0267-0, 2002.

Tunnicliffe, V.: Breakage and propagation of the stony coral Acropora cervicornis, Proc. Natl. Acad. Sci., 78, 2427–2431, https://doi.org/10.1073/pnas.78.4.2427, 1981.

Viehman, T. S.: Coral Decline and Reef Habitat Loss in the Caribbean: Modeling Abiotic Limitations on Coral Populations and Communities, Dissertation, Duke University, https://hdl.handle.net/10161/14407 (last access: 23 October 2023) 2017.

Viehman, T. S., Hench, J. L., Griffin, S. P., Malhotra, A., Egan, K., and Halpin, P. N.: Understanding differential patterns in coral reef recovery: chronic hydrodynamic disturbance as a limiting mechanism for coral colonization, Mar. Ecol. Prog. Ser., 605, 135–150, 2018.

Wolfe, K., Kenyon, T. M., Desbiens, A., de la Motte, K., and Mumby, P. J.: Hierarchical drivers of cryptic biodiversity on coral reefs, Ecol. Monogr., 93, 1–27, https://doi.org/10.1002/ecm.1586, 2023.

Woodley, J. D., Chornesky, E. A., Clifford, P. A., Jackson, J. B. C., Kaufman, L. S., Knowlton, N., Lang, J. C., Pearson, M. P., Porter, J. W., Rooney, M. C., Rylaarsdam, K. W., Tunnicliffe, V. J., Wahle, C. M., Wulff, J. L., Curtis, A. S. G., and Dallmeyer, B. P.: Hurricane Allen's impact on Jamaican coral reefs, Science, 214, 749–755, 1981a.

Woodley, J. D., Chornesky, E. A., Clifford, P. A., Jackson, J. B. C., Kaufman, L. S., Knowlton, N., Lang, J. C., Pearson, M. P., Porter, J. W., Rooney, M. C., Rylaarsdam, K. W., Tunnicliffe, V. J., Wahle, C. M., Wulff, J. L., Curtis, A. S. G., Dallmeyer, M. D., Jupp, B. P., Koehl, M. A. R., Neigel, J., and Sides, E. M.: Hurricane Allen's impact on Jamaican coral reefs, Science, 214, 749–755, https://doi.org/10.1126/science.214.4522.749, 1981b.

Young, I. R.: Seasonal Variability of the Global Ocean Wind and Wave Climate, Int. J. Clim., 19, 931–950, https://doi.org/10.1002/(SICI)1097-0088(199907)19, 1999.

Yu, K., Zhao, J., Roff, G., Lybolt, M., Feng, Y., Clark, T., and Li, S.: High-precision U-series ages of transported coral blocks on Heron Reef (southern Great Barrier Reef) and storm activity during the past century, Palaeogeogr. Palaeocl., 337–338, 23–36, https://doi.org/10.1016/j.palaeo.2012.03.023, 2012.

Zahir, H., Quinn, N., and Cargilia, N.: Assessment of Maldivian Coral Reefs in 2009 after Natural Disasters, Male', Marine Research Centre of the Ministry of Fisheries Agriculture and Marine Resources Male' http://www.mrc.gov.mv/assets/Uploads/October-2009-Assessment-of-Maldivian-Coral-Reefs-in-2009 (last access: 23 October 2023), 2009.